Mansoura Engineering Journal

Volume 37 | Issue 2 Article 8

6-1-2021

Effect of Bentonite Mud Additives on Flow Structure and Cuttings Transport through the Eccentric Annulus of Wellbore.

Mohamed Sakr
PhD Student of Mechanical Power Engineering Department., Faculty of Engineering., El-Mansoura University., Mansoura., Egypt., mlsakr@mns.com

Ahmed Sultan
Professor of Mechanical Power Engineering Department., Faculty of Engineering., El-Mansoura University., Mansoura., Egypt.

M. Tolba
Mechanical Engineering Department., Faculty of Engineering., El-Mansoura University., Mansoura., Egypt.

M. Badawy
Former Head of AlAlamin Oil Company., Egypt

Recommended Citation

Sakr, Mohamed; Sultan, Ahmed; Tolba, M.; and Badawy, M. (2021) "Effect of Bentonite Mud Additives on Flow Structure and Cuttings Transport through the Eccentric Annulus of Wellbore.," *Mansoura Engineering Journal*: Vol. 37 : Iss. 2 , Article 8.
Available at: https://doi.org/10.21608/bfemu.2012.120611

Effect of Bentonite Mud Additives on Flow Structure and Cuttings Transport through the Eccentric Annulus of Wellbore

تأثير إضافات طين الحفر على هيكل السريان وكفاءة نقل نواتج الحفر فى المجري الحلقى الغير متمركز لثقب الحفر

by

Mohamed L. H. Sakr[1], A. A. Sultan[2], M. A. Tolba[2], and M. A. Badawy[3]

[1] PhD student, Mechanical Engineering Dept, Mansoura Univ., Mansoura, Egypt.
Mlsakr@msn.com

[2] Mechanical Engineering Dept, Mansoura Univ., Mansoura, Egypt

[3] Former head of Al Alamin Oil Co., Egypt

Abstract

The effect of bentonite mud additives on flow structure and cuttings transport efficiency through drill hole (wellbore) eccentric annular flow is studied numerically and presented in this work. Velocity distribution profiles and contours of both drilling fluid and cuttings are examined in the presence of drill pipe rotation. Cuttings volume fraction distributions as well as flow contours is considered. The effect of additives on the cuttings slip velocity and transportation efficiency is studied. *Potassium chloride (KCl) and potassium formate (KF)*, as wellbore stability, and viscosity control additives are investigated. *PG gum* as bentonite mud additive for filtration, viscosity, and gel strength control as well as barite additive to control mud density is studied.

The study is carried out using Fluent 6.3.26 package CFD software. The turbulent model considered is the realizable k–ε model. Flow passage considered is an eccentric annulus that has inner and outer diameters of 5 cm and 10 cm with 50% eccentricity, and length L=500 cm. Base fluid considered is 4.3% bentonite mud. 3% bentonite mud is also investigated with *PG gum* additives. Drilling fluid rheological model considered is the power law. Results show that the axial, velocity distributions of both drilling fluids and cuttings, as well as, drilled cuttings volumetric fraction distribution are strongly affected by drilling fluid additives. Additives modify the flow structure and cuttings distribution, and the effect depends on drilling fluid's rheology as represented by their viscosities. Bentonite mud additives reduce cuttings slip and increase cuttings transport efficiency.

الملخص:

تقدم هذه الورقة دراسة عددية لتأثير بعض المواد المضافة لطين الحفر لتحسين فعاليته على هيكل السريان ثنائى الطور لسوائل ونواتج الحفر، وتأثير هذه الاضافات على كفاءة نقل نواتج الحفر فى المجري الحلقى غير المتمركز لثقب الحفر. حيث تم دراسة توزيع السرعة لكل من سوائل ونواتج الحفر كل على حده وتركيز نواتج الحفر على المقطع. تم دراسة تأثير عدد من الاضافات المستخدمة لتحسين خواص طين البنتونيت كسائل حفر، حيث تم دراسة تأثير املاح البوتاسيوم (كلوريد وسلفات البوتاسيوم *KCl and KF*)، كما تم دراسة تأثير مادة *PG gum* ومادة البريت.

أجريت الدراسة على السريان ثنائى الطور لسوائل ونوتج الحفر فى مجري حلقى غير متمركز طوله ٥٠٠ سم وقطر خارجى ١٠سم وداخلى ٥ سم، ٥٠% لامركزية. وتم استخدام حزمة البرمجيات Fluent 6.3.26 لحل معادلات الحركة للسريان ثنائى الطور المضطرب واستخدام نموذج الاضطراب realizable k–ε model، كما تم استخدام النموذج الأسي power law للتعبير عن ريولوجيا سوائل الحفر. وتوضح نتائج هذا البحث أن المواد المضافة إلى سوائل الحفر تؤثر وبشكل كبير على سرعة كل من سوائل ونواتج الحفر وتوزيعها على المقطع، كما تؤثر على توزيع تركيز نواتج الحفر على المقطع، وأن هذه الاضافات تؤدي الى التقليل من انزلاق نواتج الحفر تحت تأثير الوزن وبالتالي ترفع من كفاءة سوائل الحفر الى نقل نواتج الحفر فى ثقب الحفر، كما تؤكد النتائج أن تأثير هذه الاضافات ناتج عن تحكمها في ريولوجيا سوائل الحفر وبصفة خاصة اللزوجة

Accepted June 30, 2012

1. Introduction

Drilled cuttings are transported upwards by the drilling fluid through the annular space between the drillpipe and wall of the drill hole. Cuttings transport is the most important factor that affect hole cleaning and drilling operations efficiency. The transport of cuttings by drilling fluids through the drill hole is mostly affected by drilling fluid properties. Optimization of drilling hydraulics design requires good understanding of cuttings transport.

The basic properties of drilling fluids are fluid density, fluid viscosity and gel strength. Drilling fluid viscosity must be high enough to remove cuttings generated by the drill bit and other formation material that may fall into the wellbore. Drilling fluids are normally shear thinning, having apparent viscosity decreasing with increasing shear rate. Fluids must have sufficient gel strength to suspend rock cuttings under static well conditions.

Drilling fluids have a natural tendency to flow into permeable formations because the borehole pressure is generally higher than that in the formation. To prevent excessive leak-off, a thin, low permeability filter cake is formed using additives. One of the most fundamental functions of a drilling fluid is to exert adequate hydrostatic pressure in the wellbore to balance formation pressures and to prevent uncontrolled influx of formation fluids that may result in a blowout. Drilling mud density must be controlled accurately by suitable weighting material additives.

Water based muds such as bentonite clays, oil-based muds and polymer-viscosified fluids are often used as drilling fluid. The most important commercial clays used for increasing the viscosity of drilling fluids are bentonite, attapulgite, and sepiolite. Bentonite concentrations in drilling fluids vary widely up to 100 kg/m^3 (35 lb/bbl). There are many drilling fluid additives which are used to develop the key properties of the drilling mud. Barite ($BaSO_4$), hematite (Fe_2O_3), magnetite (Fe_3O_4), and sodium chloride (NaCl) are widely used as weighting material additives to control mud density.

The rheological properties are adjusted using inorganic and organic additives to achieve the cuttings carrying capacity of drilling fluid and generate adequate bit hydraulic horsepower for fast drilling at moderate flow rates. The viscosity of the drilling fluid determines the cuttings carrying capacity of the fluid. The exact representation of this property differs depending on the type of fluid and the rheological model being used for the evaluation of the fluid parameters.

It has been recognized that drilling fluids rheology greatly affects the flow structure and transport process of drilled cuttings in the drilling pipe. Many rheological models have been developed to represent the non Newtonian characteristics and behavior of drilling fluids. Lauzon and Reid (1979) carried out rheological classifications of drilling fluids. They proved that the power-law model is more than accurate for all

shear-rate ranges encountered in drilling operations but not for the extremely high such as those that occur across drill-bit nozzles.

Piggott (1941) was the first to study of the mud flow in pipes, wellbores, and mud pits. He presented the results of drilling mud hydraulics in the pipe and annulus. He concluded that raising mud velocity and density was most beneficial for cuttings removal, and high viscosity either in laminar or turbulent flow was undesirable. Clay concentration has significant effect on pressure loss in laminar flow. But for turbulent flow, a little more pressure loss was observed due to the presence of clay. In addition, Piggott stated that 5% cuttings concentration in the drilling fluid is safe for cuttings transport. Vinod (1994) carried out numerical study to discuss the fact that fluids rheology is the determining factor in the efficiency of the transport of drill bit cuttings. Results show that power law index is a significant parameter in determining the local flow regime in the different regions of the annulus. Hence, accurate control of power law index is critical in optimizing bore hole flow.

Sifferman, et. al. (1973) carried out experimental study in oil field derrick with casing to drill pipe diameter ratio 12 in./3.5 in., using four different mud weights (10-15 ppg), and three cutting sizes of simulated chips (dp=0.0625-0.25 in.). They reported that cutting transport efficiency increases as fluid viscosity increases. Hussain et. al. (1983) carried out experimental study of cutting transport in annulus with inner and outer diameters of 1.2 in. and 5 in. and 50.2 ft length. Muds considered are (1) flocculated gel system (*bentonite, KCl*), (2) gel/polymer system (*bentonite, XC/Polymer, Caustic soda*), and (3) gel/chemical system [*bentonite, Peltex (ferrochrome lignosulfate), caustic soda*] with two cutting sizes. The results showed that increases in both the annular fluid velocity and yield point were favorable to faster cutting transportation, and hence, efficient hole cleaning.

Belavadi and Chukwu (1994) studied experimentally the flow in casing-drill pipe annulus using four different weights of bentonite muds (8.9-13 ppg), with cutting chips of graded sizes small, medium and large were investigated. They found that increase in the flow rate at higher fluid densities greatly increase the transport ratio. This effect is almost negligible when using low density fluids to transport large size cuttings. They reported that the fluid density to viscosity ratio concept controls cuttings transport. Walker and Li (2000) investigated particles transport in an annulus flow loop using three different muds of HEC, Xanvis polymer and water with particle sizes dp=0.15-7.0 mm. Results show that fluid rheology plays an important role for solid transport and to achieve optimum results for wellbore cleaning, the best way to pick up solids is with a low viscosity fluid in turbulent flow but to maximize the carrying capacity a gel or a multiphase system should be used to transport the solids out of the well bore.

Velocity distributions of Newtonian and non-Newtonian fluids in eccentric annuli are considered in several publications. It should be noted that all the studies previously discussed considered velocity profiles with only liquid flowing inside the eccentric annulus. Effects of solid particles in the flow stream were not included. Sakr (2008), Azouz et al. (1993) and Azouz (1994) developed a single-phase model, based on the Navier-Stokes equations and later extended the model to non-Newtonian fluids, to calculate the velocity profile and the distribution of turbulent eddies in the annulus. Turbulence is thought to play an important role in dispersing the cutting.

Newitt et al. (1961) showed that the presence of solids up to 10 percent by volume had little or no effect on the velocity distribution. For concentrations over 15 percent, the velocity profile was flattened even in laminar flow. Mitsuishi and Aoyagi (1973) carried out detailed experimental study of velocity profiles in eccentric annuli. They measured velocities of non-Newtonian CMC solutions using hydrogen bubbles and showed that velocities are lower in the reduced section of an eccentric annulus, the reduction in velocity depending on eccentricity and pipe diameter ratios.

Brown et al. (1989) observed that hole cleaning was more efficient with water in turbulent flow than with hydroxyethyl cellulose (HEC) based drilling fluid. Bentonite is added in drilling fluids for viscosity control, to aid the cuttings transport and for filtration control to prevent filtration of drilling fluids into formations.

Hemphill and Larsen (1993) performed experimental study using oil-based and water-based drilling fluids. They concluded that fluid velocity and the power law index of the fluid are the significant factors affecting hole cleaning, and recommended using power law model to represent the rheology of drilling fluids. Attention was focused on prediction of the rheology effects and flow rates on drilling operations by knowing the slip velocity of the cuttings [Azar and Sanchez (1997)]. Sample and Bourgoyne (1978) developed correlations for slip velocity, related to cuttings transport efficiency in vertical wells, between fluid rheology and physical characteristics of drilled cuttings.

Yan et al (2007) studied the rheological characteristics of PG gum based drilling fluids at different concentrations and aging temperatures. The effects produced by the addition of inorganic salts (NaCl and CaCl2) on the rheological properties of PG gum based drilling fluids were also studied. The results show that PG gum based drilling fluids investigated behaves as non-Newtonian shear-thinning fluids. With the increase of *PG gum* from 0.5% to 2.5%, the consistency coefficient increases while the viscosity behavior index decreases.

Experimental studies using power law model to represent drilling fluids (CMC, Xanthan Gum, Bio-polymer (XC)) to determine the minimum transport velocities for various hole inclinations, inner pipe rotary speed and cuttings size [Ford et al. (1990), and Amundarain et al. (2009)]. Results show that hole cleaning efficiency is

dependent on the flow regime and the critical transport velocity CTV appears to pass through a maximum value for increasing viscosity.

Perez et al (2004) studied experimentally the two phase flow of Guar gum solutions and sand in the annular space of concentric-pipe system. Their results show that the addition of guar gum decreases the minimum annular velocity needed to achieve homogeneous solids distribution in the annular region. Their results also show that relatively high viscosities, high polymer relaxation times are desired rheological characteristics for a drilling fluid to obtain a uniform solids distribution in the annulus, as well as high solids carrying capacity. Mahto and Sharma (2008) stated also that rheological properties and filtration loss property of water-based drilling fluids greatly depends on the quality and quantity of the bentonite clay, as well as the additives that are used in formulations. Karagüzel et al (2010) explored the possibility of (Na, Ca)-bentonites, as an alternative to sodium bentonite, to meet the required drilling mud properties. Activation of the bentonites was performed using the most popular (Na_2CO_3) and also the most controversial additive (MgO) and their blends.

The above discussion revealed the need for studies that investigate the two phase flow structure of drilling fluids and cuttings through the eccentric annulus of drill hole, and the effect of drilling fluid additives on flow structure and cuttings transport efficiency. Therefore, it is objected to study the influence of bentonite additives upon the flow structure of drilling flow and cuttings in the wellbore eccentric annulus. The examination of their role on cutting slip velocity and cuttings transport is also aimed.

2. Problem Description

It is objected to study the influence of drilling fluid additives on the flow structure and cuttings transport efficiency of the two phase flow in drill hole annulus. The flow structure is numerically investigated in the presence of drill pipe rotation N=300 rpm. Traditionally, the annulus between the drill pipe and the borehole has been represented as eccentric annulus. The investigated eccentric annular duct has an inner diameter D_i=50 mm, outer diameter D_o=100 mm, 50% eccentricity and of length L= 500 cm. The geometry of the eccentric annulus is shown in Figure (1). Numerical simulation is carried out using the commercial software package Fluent 6.3.26. The flow is assumed to be turbulent, and computations are carried out using the realizable k–ε model.

Drilling fluids tested are bentonite (clay) based fluids. Salts were added to the fluids for wellbore stability. When drilling through shale formations, there is a tendency for the shale to absorb water from the drilling mud and swell. This leads to annular clearance reduction and can lead to stuck pipe and high torque. Hence, it is essential to increase the salt concentration in the drilling mud and lower its water activity to prevent shale's swelling. The two types of salts used in this study are potassium chloride (*KCl*) and potassium formate (*KF*). Potassium salts act as effective filtration control agent as well as viscosifier agent.

Drilling fluid test matrix is developed as in Table (1). The test matrix is formed of bentonite base fluids with *KCl, KF and PG gum* additives. Compositions are developed by varying the amounts of salt and/or viscosifier present in the fluids. Barite is added to control mud weight. Base fluid is formed by adding 15 gm of bentonite to into 350 ml of water. Caustic soda (NaOH) is added to each of the fluids for filtration control and to ensure that the pH was greater than 9 as an acidic drilling fluid may be corrosive to drilling equipment.

Drilling fluids are complex heterogeneous mixtures of fluids and additives and characterized by their non-Newtonian behavior. Drilling fluids rheology is described by many rheological models. The most commonly and widely used model in oil industry is the Power law model. It has been verified experimentally that power law model is a simple and accurate to represent the rheology of drilling fluids (Lauzon and Reid (1979)). The constitutive equation for the power law model and the apparent viscosity relation are given as.

$$\tau = K.\gamma^{n} \quad (1)$$

$$\mu_a = K.\gamma^{n-1} \quad (2)$$

K is called the *fluid consistency* and n the *flow index*. In this work the investigated fluids are bentonite-base mud, with *KCl*, *KF*, *PG gum*, and barite additives. Table (1) presents the density and the power law rheological parameters of considered drilling fluids as given by Enilari (2005).

3. Mathematical Modeling

The two phase flow of drilling fluids and cuttings in the eccentric passage of the drill hole is studied using granular-Eulerian model. The Eulerian two-phase model assumes that the flow consists of solid cuttings (*s*) and drilling fluid (*f*) phases, are separate, but form interpenetrating continua, such that he volumetric concentrations of the fluid and solid phases α_f *and* α_s are related by

$$\alpha_f + \alpha_s = 1 \quad (3)$$

The numerical model allows the determination of the pressure and velocity of the solid as well as liquid phases using the commercial CFD software FLUENT. The laws for the conservation of mass and momentum are satisfied by each phase individually. Coupling is achieved by pressure and inter-phases exchange coefficients. The conservation equations governing the two phase flow of drilling fluid and cuttings are presented in the general form as following:

3.1. *Conservation of mass*:

For solid-liquid two phase flow with no mass transfer between phases

$$\frac{\partial}{\partial t}(\alpha_q \rho_q) + \nabla.(\alpha_q \rho_q \vec{U}_q) = 0 \quad (4)$$

where $\vec{U}_q$ is the velocity of phase q (*f* or *s*)

3.2. *Conservation of momentum*

For momentum equations of the solid-liquid two phase flow, the lift force is neglected as compared to the drag force, and the virtual mass force is neglected due to the fact that it significant only when the

secondary phase density is much smaller than the primary phase density, then;

For liquid phase "f"

$$\frac{\partial}{\partial t}(\alpha_f \rho_f \vec{U}_f) + \nabla.(\alpha_f \rho_f \vec{U}_f \vec{U}_f) = -\alpha_f \nabla p + \nabla.T_f + \alpha_f \rho_f \vec{g} + K_{sf}(\vec{U}_s - \vec{U}_f) + \alpha_f \rho_f (\vec{F}_f) \quad (5)$$

For solid phase "s"

$$\frac{\partial}{\partial t}(\alpha_s \rho_s \vec{U}_s) + \nabla.(\alpha_s \rho_s \vec{U}_s \vec{U}_s) = -\alpha_s \nabla p - \nabla p_s + \nabla.T_s + \alpha_s \rho_s \vec{g} + K_{fs}(\vec{U}_f - \vec{U}_s) + \alpha_s \rho_s (\vec{F}_s) \quad (6)$$

The stress-strain tensor T_q of the liquid phase "*f*" and solid phase "*s*" is given as

$$T_q = \alpha_q \mu_q (\nabla \vec{U}_q + \nabla \vec{U}_q^T) + \alpha_q \left(\lambda_q - \frac{2}{3}\mu_q\right) \nabla.\vec{U}_q \bar{\bar{I}} \quad (7)$$

where, μ_q and λ_q are the shear and bulk viscosity of the liquid phase "*f*", or solid phase "*s*", $\vec{F}_f$ *and* $\vec{F}_s$ are external body force for liquid and solid phases, p is the pressure shared by all phases and where p_s is the solids pressure. K_{sf} *and* K_{fs} are the momentum exchange coefficient between liquid phase "*f*" and solid phase "*s*", and vise versa [Fluent (2006)]. Details of the mathematical model are given in Sakr et al (2012).

In the near wall region, the standard wall function is used. The wall function helps in more precise calculation of near-wall shear stresses for both liquid and solid phases in the Eulerian two-phase model.

No-slip boundary conditions are imposed on all the solid surfaces for the continuous phase. The same conditions are also applied to the discrete phase and imposed on the corresponding momentum equations. The inlet liquid velocity and the outlet pressure were specified. No-slip boundary conditions were assumed at the walls for the liquid phase. Interactions between the particles and the walls were modeled with the same formulation used for solids pressure and granular viscosity for the particle–particle interactions.

4. Numerical Solution

The computational grid was generated using Gambit 2.3.16. Meshing the eccentric annulus passage volume is created with 30 divisions in the radial directions, 120 divisions in the angular direction, and 100 divisions in the axial directions producing 360000 hexahedral cells. For long ducts, hexagonal shape and Cooper-type element have been employed to get better convergence and accuracy. Figure (2) presents the mesh structure of the eccentric annulus

The governing partial differential equations were discretized using finite volume technique. The discretized equations with the initial and boundary conditions were solved using Fluent 6.3.26.

Eulerian–Eulerian approach for granular flow is used, which allows the determination of the pressure and viscosity of the solids phase. Second-order upwind discretization scheme was used for the momentum equation, and QUICK discretization was used

for volume fraction, turbulent kinetic energy and turbulent dissipation energy. These schemes ensured satisfactory convergence, accuracy, and stability.

The convergence criterion is based on the residual value of the calculated variables, that is, mass, velocity components, turbulent kinetic energies, turbulent dissipation energies and volume fraction. Convergence criterion of $1x10^{-5}$ was chosen for r, θ and z velocity components, turbulent energy k, and turbulent dissipation ε of the two phases as well as the continuity equation. Convergence criteria were achieved after 1350 and up to 3500 iterations.

In pressure–velocity coupling the phase-coupled Simple algorithm was used. Other solution strategies are the reduction of under-relaxation factors of momentum, volume fraction, turbulent kinetic energy and turbulent dissipation energy to bring the nonlinear equation close to the linear equation, and subsequently using a better initial guess based on a simpler problem.

5. Results and Discussions

The influence of drilling fluid additives on flow structure and cuttings transport of the two phase flow of drilling fluids and cuttings in the eccentric annulus between the drill hole and pipe is objected. It has been discussed in a previous work [Sakr et al (2012)], that drilling fluid's viscosity plays an important role on flow structure and cuttings slip velocity. The effect of drilling fluid density on flow structure is considered. The results of the flow structure results presented in the following are those at the outlet section of the eccentric annular passage. Average flow velocity is $U_{av} \cong 1.9$ m/s, cuttings size is dp=4 - 6 mm, and cuttings to drilling fluid mass ratio is m_r=40% - 50%. Drill pipe rotation is kept constant at 300 rpm. Flow Reynolds number was varied from 100 to 150,000, where Re is defined as

$$Re = (\rho_f . U_{av} . D_h)/\mu_f$$

5.1. KCl and KF Salt Additives

Drilling fluid removes cuttings from the wellbore as drilling progresses. This process is governed by the velocity at which fluid travels up the annulus, as well as by the fluid viscosity or flow properties, and fluid density. The efficiency of cuttings removal usually increases with increasing viscosity and density. Numerous mud additives help in developing drilling fluid properties to the desired one. In fact, water-based muds have three basic components; water, reactive solids, and inert solids. The water forming the continuous phase may be freshwater, or seawater. The reactive solids are composed of commercial clays, incorporates hydrate-able clays, and polymeric materials, which may be suspended or dissolved in the water phase.

The most important commercial clays used for increasing the viscosity of drilling fluids are bentonite, attapulgite, and sepiolite. Standard API bentonite is almost processed bentonite using small amount of polymer to enhance the viscosity building properties of the clay. There are many drilling fluid additives which are used to develop the key properties of the drilling

mud. Potassium salts are added to the bentonite base fluids for wellbore stability and viscosity control. In this work, potassium chloride (*KCl*) and potassium formate (*KF*) as additives to bentonite base fluids are investigated. Barite is added to drilling fluids to control its density. Caustic soda (*NaOH*) or lime is added to drilling fluids in order to ensure that the pH is greater than 9 as an acidic drilling fluid may be corrosive to drilling equipment. The power law rheological model parameters of these fluids are given in table (1-a)

The effect of potassium salts on flow structure at the outlet cross section of the eccentric annulus of L=500 cm is shown in figures (3)-(9). Drilling fluids considered are bentonite base fluid with *KCl* and *KF* additives at an average velocity $U_{av} = 1.9\ m/s$, cuttings to drilling fluid mass ratio m_r = 50%, and cuttings size dp =6 *mm*. Four *KF* and *KCl* concentrations; 0.5%, 1%, 2% and 3% are considered. Figure (3) presents typical axial velocity contours at outlet cross section of the annulus. For the flow of bentonite base fluid, the viscosity is $\mu = 0.013\ Pa.s$ and Reynolds number is Re=7760, high velocity contours region is found in the wide section with irregular shape and low velocity region exists in the narrow section. Addition of 0.5%, 1%, 2% and 3% *KCl* to the base fluid, increases the viscosity to 0.017, 0.02, 0.04, and 0.09 $Pa.s$, that corresponds to reduced values of Re to 5800, 5120, 2570, and 1130 respectively. As a result, the region of high velocity contours in the wide section becomes more regular in shape. While, increasing the percentage *of KCl* decreases the low velocity contours in the narrow region of the annulus.

The addition of 0.5%, 1%, 2% and 3% of potassium formate *KF* to the base fluid, increases the viscosity to 0.025, 0.034, 0.065, and 0.104 $Pa.s$, which is almost 50% higher than that of *KCl at the same concentration*. The corresponding flow Reynolds numbers are Re=4040, 2940, 1540, and 960 respectively. Figure (3) shows that the effect of *KF* on axial flow velocity contours are very much similar to that of *KCl*. The result demonstrates the presence of two flow structure patterns in the wide section of the annulus. Turbulent one characterized by irregular high velocity contours at high Reynolds number, and laminar flow structure characterized by narrow, sharp, and regular shape high velocity contours at low Reynolds number.

Cuttings volume fraction contours of the two phase flow of bentonite-potassium salt additive fluids and cuttings are shown in Figure (4). In general, cuttings distribution takes the form of a ring in the core region of the annulus. For the flow of bentonite base fluid, cuttings are concentrated as a ring in the middle of the annulus. The width of this ring is large in the wide section and small in the narrow section of the annulus, and the concentration is very high in the wide section. The addition of 0.5%, 1%, 2% and 3% *KCl* to the base fluid, moves the high concentration solids in the wide section towards the narrow section. The result is the appearance of a low concentration region in the wide section coming out of the narrow

one. Same cuttings volume fraction structure is found when *KF* is added to drilling fluid, but the appearance of the low concentration region in the wide section occurs at lower *KF* concentrations.

Typical plot of the normalized velocity $[\widehat{U} = u/U_{av}]$ profiles of bentonite base fluid flow with *KCl and KF* additives in the eccentric annulus is given in Figure (5-a). Velocity profiles at all sections show asymmetric distribution. At the narrow gap section P1, velocity profiles are biased to the wall of the inner rotating cylinder, while velocity profiles at the wide gap section P3 are biased to the outer wall of the annulus. Flow velocities in the wide section are higher than that in the narrow section. Almost *KCl* has no effect on velocity profiles for small concentrations up to 1.0%, but for higher concentrations, results show that the normalized velocity profiles at the wide section P3 increases with the increase of *KCl* concentration, and decreases at narrow gab section P1. However, the effect of potassium formate *KF* additives on velocity profiles is more pronounced even for small concentrations. The addition of *KF* to bentonite base fluid increases the velocity in the wide section and decreases flow velocity at other sections. This attributed to increased viscosity μ of the drilling fluid with the addition of *KCl and KF* that causes increase in flow resistance in narrow sections. Figure (5-b) presents the averaged velocity at each section P1-P4 of the eccentric annulus as function of *KCl and KF* concentration. It confirms the fact that the addition of *KCl and KF* increases drilling fluid flow velocity in the wide gap section P3, and decreases flow velocity at other sections.

The axial velocity profiles of drilled cuttings in the two phase flow through the eccentric annulus are shown in Figure (6-a). Cuttings velocity profiles are presented at sections P1 and P3. In the narrow section P1, cuttings profiles exhibit distinct peak with asymmetric distribution and are lower than that in the wide gap section. However, velocity profiles at the wide section P3 show turbulent distribution characteristics, with flat peaks asymmetric towards the outer wall of the annulus. They also exhibit higher velocities almost more than double that in the narrow section. Similar to fluid's velocity profiles reported in Figure (5) the addition of *KCl and KF* increases the cuttings velocity in the wide section P3, and reduces the cuttings velocity in the narrow one P1. It is clearly confirmed in Figure (6-b), where averaged cuttings velocities at each of sections P1-P4 are presented as function of *KCl* and *KF* concentrations.

Comparison between cuttings velocity profiles and that of drilling fluid is shown in Figure (7-a) for the two phase flow of drilled cuttings and bentonite base fluid with *KCl and KF* additives. Flow conditions are the same as those presented in figures (5) and (6). Results show that cuttings velocities are lower than that of drilling fluid especially close to the walls. This is due to the fact that low fluid velocity near the wall has low carrying capacity of cuttings. The addition of *KCl or KF* to the flow increases the axial velocity of cuttings to approach

drilling fluid velocity, especially in the core region of the flow. For the case of the flow with 2% or 3% of *KCl or KF,* it is hardly to detect any difference between the velocity of cuttings and that of the fluid in the core flow region.

It has been experimentally verified that the carrying capacity of drilling fluids are greatly affected by fluid velocity, and mud rheology, and that there is a minimum transport velocity for the drilling fluid to be able to carry cuttings [Tomren et al. (1986), and Ford et al. (1990)]. The ratio of the averaged velocity of cuttings and fluid at each section (P1-P4) is shown in Figure (7-b). The cutting to fluid average velocity ratio U_r ($U_r = u_c/U_{av}$), which is a measure of the transportation efficiency is the highest in the wide section and the lowest in the narrow section of the annulus. It also shows that the addition of *KCl and KF* to bentonite mud increases the cuttings to fluid velocity ratio U_r i.e. increases the cuttings transport ratio.

The difference between local fluid velocity u and that of cuttings u_c which is known as local cuttings slip velocity v_s, [$v_s = u - u_c$]. The slip velocity is normalized by fluid average velocity U_{av} to give $\hat{V}_s$ [$\hat{V}_s = v_s/U_{av}$] and plotted in Figure (8-a). Normalized slip velocity profiles of cuttings exhibit two peaks near the inner and outer walls of the annulus, and minimum in the core area. In general, $\hat{V}_s$ is large in the narrow section as compared to that in the wide section. This is due to low velocities in the narrow section. The addition of *KCl or KF* to bentonite base fluid reduces the slip velocity profiles in all sections. This is due to increased viscosity of drilling fluid with the addition of *KCl and KF*, cuttings slip velocity decreases. Figure (8-b) presents the averaged slip velocity at sections P1-P4 as function of *KCl and KF* additive concentration. Average values of $\hat{V}_s$ is large at the narrow section and low at the wide section for all *KCl and KF* concentrations. It has been recognized that increasing *KCl and KF* decrease of the cuttings slip velocity.

The volume fraction profiles of cuttings in the eccentric annulus flow of bentonite base fluid with *KCl and KF* additives are shown in Figure (9-a). Profiles exhibit sharp peak at the middle area of each section. The addition of *KCl and KF* increases these peaks at sections *P1, P2*, and *P4.* But it decreases the peaks of cuttings concentration at the wide section *P3* such that profiles exhibit almost flat distribution with two peaks for higher *KCl or KF* values. The concentration of cuttings is very low near the inner and outer walls of the annulus. The averaged cuttings volume fraction at *P1-P4* is plotted in Figure (9-b). It shows that cuttings volume fraction increases with *KCl and KF*, at sections, *P1, P2,* and *P4,* and decreases with *KCl and KF* at the wide section *P3*. This demonstrates that the addition of *KCl and KF* to bentonite muds makes leads drilled cuttings to be uniformly distributed

5.2 PG gum Polymeric Additives

Combination of bentonite clay and an organic thinner provides filtration control in many water-based muds. Shear thinning additives develop the rheological behavior

of drilling fluid. They can suspend drilling cuttings at low shear rates, but offer little resistance to flow at high shear rates. Synthesized polymers are commonly used to control the rheology and filtrate loss required for water-based drilling fluids. Xanthan gum was a most conventional natural polymer used to improve the rheological properties of drilling fluids, but the price of Xanthan is expensive [Amundarain et al. (2009)]. The tree gum, namely PG gum, which is mainly composed of natural hetero-polysaccharides as drilling fluid additives has been attracted much attention in the international petroleum industry in recent years. It greatly enhances the gel strength of drilling fluids required for carrying cuttings during drilling process, and acts as a good viscosifier and fluid loss control agent. In this work PG gum added to 3% bentonite-water mud is investigated to study its effect on rheological behavior and flow structure in eccentric annulus. The power law rheological model parameters of the 3% bentonite and PG gum additives are given in table (1-b) [Yan et al (2007)].

The effect of *PG gum* polymers on the flow structure at outlet of eccentric annulus of the two phase flow of cuttings and bentonite mud is presented in figures (10)-(14). Drilling fluids considered are 3% bentonite-water muds with *PG gum* additives at an average velocity $U_{av} = 1.9\ m/s$, cuttings to drilling fluid mass ratio m_r = 40%, and cuttings size dp =4 *mm*. Five *PG gum* concentrations; 0.5%, 1%, 1.5%, 2% and 2.5% are investigated.

Figure (10) presents the axial velocity and cuttings volume fraction contours at flow outlet cross section annulus of 3% bentonite-water muds with *PG gum* additives. The viscosity of 3% bentonite-water mud flow is $\mu = 0.013\ Pa.s$ and Reynolds number is Re=7400. For this fluid flow, the high velocity contours region is found in the wide gap section with irregular shape and low velocity region exists in the narrow section. The addition of 0.5%, 1%, 1.5%, 2% and 2.5% *PG gum* to bentonite mud, increases the viscosity to 0.025, 0.044, 0.081, 0.108 and 0.125, that corresponds to reducing flow Reynolds number to 3790, 2170, 1180, 890 and 770 respectively. As a result, the high velocity contours region in the wide section becomes more regular in shape with increased *PG gum* concentration, and decreases the low velocity contours in the narrow gap region of the annulus. Figure (10-a) confirmed the presence of two flow patterns, turbulent one for 0.5% *PG gum* (*Re=3790*) which is characterized by irregular shape high velocity region in the wide section. The other is laminar one as represented by the case 2.5% *PG gum* (*Re=770*) that is characterized by regular and well defined high velocity region in the wide section. In the narrow section, the reduced velocity is attributed to increased flow resistance drilling mud with polymer additives.

Cuttings volume fraction contours at the outlet cross section annulus of *PG gum* additives to bentonite mud is also shown in Figure (10-b). In bentonite mud flow with no additives, cuttings accumulate in the

wide section with high concentrations. The addition of *PG gum* makes cuttings to form a ring in the core region in the middle of annulus cross section. The width of that ring in the wide section is much larger than that in the narrow section. The increase of polymer concentration has no noticeable effect on cuttings contours.

The normalized velocity $\hat{U}$ profiles of 3% bentonite-water mud with *PG gum* additives flow in the eccentric annulus is given in Figure (11-a). Profiles presented are at sections P1and P3. Similar to the results of *KCl and KF* additives, velocity profiles show asymmetric distribution. At the narrow gap section P1, velocity profiles are biased to the wall of the inner rotation cylinder, while velocity profiles at the wide section P3 are biased to the outer wall of the annulus. Flow velocities in the wide section are much higher than that in the narrow section. Increasing the percentage of *PG gum* increases the viscosity μ and reduces Reynolds number *Re*. As a result, the velocity in the wide gap section increases and it decreases in the narrow section. This is clearly demonstrated in Figure (11-c) when the averaged velocity at each section is plotted as function of *PG gum* concentration.

Figure (11-b) presents plot of normalized axial velocity profiles of drilled cuttings in the eccentric annulus, at sections P1 and P3. In the narrow section, cuttings profiles exhibit distinct peaks in the core and has the lowest velocity values compared to that in the wide section. Increasing *PG gum* reduces the normalized velocity and makes the velocity in the core to be more flat. At the wide section *P3* of the annulus, velocity profiles have asymmetric distribution towards the outer wall of the annulus and have almost flat core distribution. It also exhibit higher velocities of more than double that in the narrow section. Similar to fluid velocity profiles reported in Figure (11-a) the addition of *PG gum* increases cuttings velocity in the wide section P3, and reduces the cuttings velocity in the narrow and other sections *P1* as demonstrated in Figure (11-b).

Comparison between the cuttings velocity profiles and that of drilling fluid is shown in Figure (12) for bentonite mud flow with *PG gum* additives. Results show that cuttings velocities are lower than that of drilling fluid especially close to the walls. The difference between fluid velocity and that of cuttings is large in the narrow section as compared to that of the wide section and others. Similar to *KCl and KF* additives, the addition of *PG gum* to bentonite mud increases the axial velocity of cuttings to approach drilling fluid velocity, in the core region of the flow. It is hardly to detect any difference between the velocity of cuttings and that of the fluid at low 0.5% *PG gum*.

The ratio of the averaged velocity of cuttings to that fluid at each section is shown in Figure (12-b). The cutting to fluid average velocity ratio U_r, as a measure of the transportation efficiency is the highest in the wide section and the lowest in the narrow section of the annulus. Figure (12-b) also shows that U_r increases with the increase of the *PG gum* additives

Cuttings normalized slip velocity $\hat{V}_s$ plotted in Figure (13-a) shows that slip velocity profiles exhibits two peaks near the inner and outer walls of the annulus, and minimum in the core area. In general, $\hat{V}_s$ is large in the narrow section as compared with that in the wide section. This is due to the low velocities in the narrow section. The addition of *PG gum* to bentonite mud greatly reduces the slip velocity. It is thought to be due to increased viscosity of with *PG gum* additives. Figure (13-b) shows the effect of *PG gum* on average slip velocity at each section of the annulus. Average values of $\hat{V}_s$ is large at the narrow section and low at the wide section for all *PG gum* concentrations. It has been recognized that increasing *PG gum* decrease of the cuttings slip velocity.

The volume fraction profiles of cuttings in the eccentric annulus outlet cross section for the flow of bentonite mud with *PG gum* additives are shown in Figure (14). Profiles exhibit sharp peak at the middle of each section. The addition of *PG gum* decreases cuttings peaks at the wide section *P3* such that profiles exhibit almost flat distribution with two peaks for higher *PG gum* values, and increases these peaks at the narrow one. The concentration of cuttings is very low near the inner and outer walls of the annulus.

5.3 Bentonite Muds with Barite Additives

Mud density must be controlled by suitable weighting materials that do not adversely affect other properties. Most important is the specific gravity of the weighting agent as well as its insolubility in water and its chemical inertness. Barite (barium sulfate $BaSO_4$) meets the overall requirements for weighting material better than other materials and is used for increasing the density of drilling fluids throughout the world.

The effect of barite additives to bentonite mud on the flow structure of eccentric annulus is investigated. Two cases are considered, one is adding barite to increase the density to 9 ppg (1078 kg/m^3), and the other is to add barite to increase fluid density to 14 ppg (1677 kg/m^3). The power law rheological model parameters of the base fluid with barite additives are given in table (1-a) [Enilari (2005)]. Three sets of bentonite muds are studied; bentonite base fluid, 0.5%*KCl* base fluid, and 0.5%*KF* base fluid. Numerical experiments are carried out at average flow velocity $U_{av} = 1.9\ m/s$, cuttings to fluid mass ratio mr =50%, and cuttings size dp =6 mm.

The effect of barite on the flow structure at outlet of eccentric annulus is presented in figures (15)-(18). Typical example for the effect of barite additive on axial velocity contours and cuttings volume fraction contours at outlet cross section is shown in Figure (15) for 0.5%*KF* bentonite muds flow. For the bentonite base fluid with 0.5%*KF*, the viscosity is $\mu = 0.025\ Pa.s$, and Re is 4040. Adding barite to adjust mud density to 9 ppg, the viscosity increases to 0.04 that corresponds to Re=2500, which is a turbulent flow, giving irregular shape high velocity region in the wide section. Increasing barite to adjust mud density to 14 ppg, the viscosity increases to 0.08 that

corresponds to Re=1370, which is a laminar flow, and shows well defined regular shape high velocity contours in the wide section. Same results are found for the case of bentonite base fluid and 0.5%*KCl* bentonite mud [see Figure (15-a)].

Typical contours of cuttings volume fraction for 0.5%*KF* bentonite mud with barite additives is shown in Figure (15-b). In bentonite base fluid flow cuttings accumulate in the form of a ring in the core region of the annulus. The width of this ring is large in the wide section and small in the narrow section of the annulus, and the concentration is very high in the wide section. For the 0.5% *KF* bentonite mud with 9 ppg barite, high concentration region in the wide section moves towards the narrow section that results in appearance of low concentration region in the wide section coming out of the narrow one. For the 14 ppg case, cuttings contours exhibits wider peak region that shifted towards the narrow section.

The normalized axial velocity $\hat{U}$ profiles of the flow of *KCl and KF* bentonite mud with *barite* additives in the eccentric annulus are given in Figure (16-a). Flow velocities in the wide section are much higher than that in the narrow section for all cases studied. Increasing barite additives increases the viscosity μ and reduces Reynolds number *Re*. As a result the velocity increases in the wide section and decreases in other sections. This is clearly demonstrated in Figure (16-c) when the averaged velocity at each section is plotted as function of drilling fluid viscosity. Normalized axial velocity $\hat{U}$ profiles of *KF bentonite* muds exhibit higher values than that of *KCl bentonite* muds which are higher than that of *bentonite base fluid* in the wide section. Whereas in other sections, the velocity of base fluid is higher, followed by *KCl* and the lowest is for *KF* bentonite mud. Figure (16-b) presents plot of normalized axial velocity profiles of drilled cuttings in the eccentric annulus for the flow of *KCl and KF* bentonite mud with barite additives. The addition of *barite* to increase mud density increases cuttings velocity in the wide section P3, and reduces the cuttings velocity in the narrow section. The average velocity of cuttings at each section shows that the velocity in the wide section increases with barite addition and decreases in other sections as shown in Figure (16-c).

Typical plot of cuttings velocity profiles and that of drilling fluid are shown in Figure (17-a) for the flow of 0.5% *KCl* bentonite mud with barite additive. For the case of 0.5% *KCl bentonite* with barite additives to 9 ppg, the difference between fluid velocity and that of cuttings is large in the narrow section as compared to that of the wide section and others. Increasing barite additive to increase mud density to 14 ppg, cuttings velocity increases to approach drilling fluid density, such that, cuttings velocity is almost the same as fluid velocity. Very similar flow structure is found for the addition of barite to 0.5% *KF* but with higher cuttings velocities due to increased viscosity of drilling fluid. The ratios of the averaged velocity of cuttings to that of drilling fluid U_r at each section are shown in Figure (17-

c). The cutting to fluid average velocity ratio U_r, which is a measure of the cuttings transportation efficiency is the highest in the wide section and the lowest in the narrow section of the annulus. It increases with mud viscosity due to *barite* additives. It is interested to note that U_r is higher for *KF* bentonite mud than that of *KCl* bentonite and base fluid muds.

Cuttings normalized slip velocity $\hat{V}_s$ plotted in Figure (17-b) shows that slip velocity profiles exhibits two peaks near the inner and outer walls of the annulus, and a minimum in the core area. In general, $\hat{V}_s$ is large in the narrow section as compared with that in the wide section. This is due to the low velocities in the narrow section. The addition of *barite* to bentonite muds greatly reduces the slip velocity. It is thought to be due to increased viscosity of the bentonite muds with *barite* additives. Figure (17-c) shows the effect of *barite* on average slip velocity at each section. Average values of $\hat{V}_s$ is large at the narrow section and low at the wide section. Increasing *barite* additives, increases mud viscosity and decrease of the cuttings slip velocity.

The effect of barite on volume fraction profiles of cuttings is shown in Figure (18). Profiles exhibit sharp peak at the middle of each section. The addition of *barite* decreases cuttings volume fraction peaks at the wide section *P3* such that profiles exhibit almost flat distribution with two peaks for 0.5% *KCl* and 0.5% *KF* bentonite muds with 14 ppg barite additives. Barite increases these peaks at other sections. Cuttings concentration is very low near the inner and outer walls of the annulus.

5.4 Cuttings Slip and Transportation

Cuttings slip velocity V_s is the difference between fluid velocity and cuttings velocity. The slip velocity is an indication of transport deficiency of drilled cuttings particles. In fact, cuttings velocity is the results of viscous forces of drilling fluid flow that forces the cuttings to move up with the flow, and the gravity force due to cuttings mass density that drags cuttings down in opposite to flow direction. Cutting transport ratio is defined as the ratio of net axial cutting velocity and fluid axial velocity. It is a measure of the transportation efficiency η_t, and may be expressed as, $\eta_t = U_c/U_{av}$

In the aforementioned discussion, drilling fluid additives to bentonite mud affect the structure of the two phase flow. It has been demonstrated that *KCl, KF, PG gum and barite* additives decrease cuttings slip velocity and increase cuttings to fluid velocity ratio. In this work, the slip velocity of drilled cuttings is calculated as the difference between area weighted averaging of fluid velocity and cuttings velocity over the outlet cross sectional area of the annulus $[V_s = (U_{av} - U_c)]$. The slip velocity is normalized by fluid's average velocity U_{av} to give $\hat{V}_s$ $[\hat{V}_s = V_s/U_{av}]$. The results are presented in Figure (19-a) as function of additive concentration. It shows that the slip velocity $\hat{V}_s$ decreases with *KCl, KF, and PG gum* additives, and $\hat{V}_s$ is larger for cuttings diameter dp=6 mm than that of dp=4 mm. Figure (19-b) presents the effect of additives

on cuttings transport ratio η_t showing that *KCl, KF, and PG gum* drilling fluids additives increase transport efficiency. Cuttings with smaller diameter (dp=4 mm) have higher cuttings transport efficiency than larger one (dp=6 mm), and *PG gum* additive is more efficient in cuttings transportation. It is very interesting to find that all results of normalized slip velocity of cuttings with same diameter fall on a single curve when plotted as function of drilling fluid viscosity, as shown in Figure (20-a) and can be best fitted by the relation

$$\hat{V}_s = 0.011(\mu)^{-0.63} \quad \text{for } dp\text{=6 mm,}$$

$$\hat{V}_s = 0.005(\mu)^{-0.68} \quad \text{for } dp\text{=4 mm}$$

Similar results are found for cuttings transport ratio η_t when plotted as function of viscosity as shown in Figure (20-b).

5.5. *Pressure Loss and Friction Coefficient*

The influence of bentonite mud additives upon the pressure loss, and friction coefficient of the two phase flow in drilling hole eccentric annulus is studied. The pressure loss gradient and coefficient inside the annulus using power law rheological model are shown in Figure (21) and (22) as function of Reynolds number. The results are compared with single phase flow at the same conditions, and the friction coefficient of single phase flow is compared with available experimental data in literatures.

Figure (21) presents the results of friction coefficient C_f of the single phase flow of bentonite base drilling fluids in the eccentric annulus as function of Reynolds number Re. It is very interesting to find that all the results of the numerical experiments fall on a single curve as shown in figure (21-a). Two patterns are found, the first one is for laminar flow of high viscous fluids and low Reynolds numbers up to 2,000, where, the friction coefficient C_f is best fitted by the power law relationship as

$$C_f = 10/Re^{0.8} \qquad (8\text{-a})$$

The other pattern is that for low viscosity fluids and high Reynolds numbers, where friction coefficient C_f is best fitted by the well known relation.

$$C_f = 0.079/Re^{0.25} \qquad (8\text{-b})$$

Figure (21-b) presents comparison between the results of the friction coefficient C_f of the single phase flow in the eccentric annulus and available experimental data [Okafor and Evens (1992), Langligais et al (1983), Han et al (2010), Fordham et al. (1991), Pilehvari and Serth (2009), Ogugbue (2009), and Hansen et al. (1999)]. The agreement is good.

Figure (22) presents the results of friction coefficient C_f of the two phase flow of drilled cuttings and bentonite base drilling fluids in the eccentric annulus as function of Reynolds number Re. In comparison with single phase results, it is clear the friction coefficient of two phase flow is higher than that of single phase. However, for high viscosity fluids and low Re flows, the friction coefficient of two phase flow approaches the values of single phase one. This is highly dependent on cuttings size, volume fraction and flow velocity.

6. Conclusions

This work presents a numerical study for the effect of bentonite mud additives on the two phase flow structure and characteristics of drilled cuttings and fluid in eccentric annulus. The influence of *KF* and *KCl* salt additives, and *barite* as well as *PG gum* polymer additives are investigated. The following are concluded:

1. The addition of *potassium chloride KCl, potassium formate KF, PG gum and barite* to bentonite mud, increases the viscosity and reduces flow Reynolds number.
2. Velocity contours exhibits region of high velocity contours of irregular shape in the wide gap that becomes more regular in shape with drilling fluid additives.
3. Two flow patterns in the wide gap of the annulus are found. Turbulent one of irregular high velocity contours and flat velocity profiles at high Reynolds number. The other is laminar characterized by sharp, well defined and regular shape high velocity contours, and parabolic velocity profile at low Reynolds number.
4. Velocity profiles of drilling fluids as well as drilled cuttings exhibit higher values at the wide section than that in the narrow section. The addition of *KCl, KF and PG gum* to bentonite mud increases the velocity in the wide section and decreases in other sections.
5. Cuttings velocities are lower than that of drilling fluid especially close to the walls. The addition of *KCl, KF, and PG gum* to bentonite mud increases the axial velocity of cuttings to approach that of drilling in the core region of the flow.
6. Cuttings/Fluid velocity ratio, which is a measure of the cuttings transport efficiency, increases with additives.
7. Cuttings slip velocity $\hat{V}_s$ profiles exhibit two peaks near the inner and outer walls of the annulus. $\hat{V}_s$ is large in the narrow section as compared with that in the wide section. This is due to low velocities in the narrow section. Bentonite mud additives reduce the cuttings slip velocity profiles.
8. Cuttings are concentrated as a ring in the middle of the annulus with large width in the wide section and small in the narrow section. The mud additives move high concentration solids in the wide section towards the narrow section. This results in the appearance of a low concentration region in the wide section coming out of the narrow one.
9. Normalized slip velocity of cuttings, and cuttings transport ratio are function of fluid's viscosity. For same cuttings diameter, all results of slip velocity and cuttings transport ratio fall on a single curve when plotted as function of drilling fluid viscosity.
10. Normalized slip velocity $\hat{V}_s$ decreases with KCl, KF, PG gum and barite additives, and $\hat{V}_s$ is larger for large cuttings diameter. They also increase cuttings transport efficiency

11. Results of the friction coefficient C_f exhibit two patterns. The first one is for laminar flow of high viscous fluids and low Reynolds numbers up to 2,000, where, C_f decreases with Reynolds number in power law relationship. Other pattern is turbulent for low viscosity fluids and high Reynolds numbers. The friction coefficient C_f of the two phase flow is higher than that of single phase one.

Nomenclature

C_f Friction coefficient,

$C_f = 2\,\tau_w/[2\rho_f\,(U_{av})^2]$

$$C_f = [\left(\frac{dp}{dx}\right) D_h]/[2\rho_f\,(U_{av})^2]$$

D_h Eccentric annulus hydraulic diameter; $D_h = (D_o - D_i)$; (m)

D_i Inner diameter of the eccentric annulus

D_o Outer diameter of the eccentric annulus

dp Cuttings particle size (mm)

dp/dx Pressure loss gradient (Pa/m)

K Power law model *fluid consistency* (Pa.s^n)

L Length of the eccentric annular passage

m_r Cuttings to drilling fluid mass ratio

n Power law model *flow index*

p Pressure shared by all phases

Re Flow Reynolds number based on drilling fluid parameters, $Re = (\rho_f . U_{av} . D_h)/\mu_f$

r_n Normalized radial distance r_n defined as: $r_n = (r - r_{min})/(r_{max} - r_{min})$

u Fluid flow velocity (m/s)

U_{av} Average drilling fluid flow velocity (m/s)

U_c Average cuttings velocity (m/s)

u_c Cuttings velocity (m/s)

V_s Average cuttings slip velocity, $V_s = (U_{av} - U_c)$ (m/s)

v_s Cuttings slip velocity, $v_s = (u - u_c)$ (m/s)

Greek Symbols

α_f Volumetric fraction of drilling fluid phase

α_s Volumetric fraction of solid phase

γ Strain rate,

τ Shear stress,

References

- Amundarain, J. L., Castro, L. J., Rojas, M. R., Siquier, S., Ramírez, N., Müller, A. J., and Sáez, A. E., "Solutions of Xanthan gum/guar gum mixtures: shear rheology, porous media flow, and solids transport in annular flow", Rheol Acta (2009) 48:491–498
- Azar, J. J. and Sanchez, R.A., "Important Issues in Cuttings Transport for Drilling Directional Wells," SPE Paper 39020 presented at the 5th Latin America and Caribbean Petroleum Engineering Conf., Rio de Janeiro, Brazil, Aug. 30 -Sept. 3, (1997).
- Azouz I., Shirazi S. A., Pilehvari Ali, and Azar J. Jamal. "Numerical simulation of laminar flow of yield-power-law fluids in conduits of arbitary cross-section", Trans. of the ASME, Journal of Fluids Engineering, 115(4): pp710-716, (1993)
- Azouz, I., "Numerical Simulation of Laminar and Turbulent Flows of Wellbore Fluids in Annular Passages of Arbitrary Cross-Section", Ph.D. Dissertation, University of Tulsa, Tulsa (1994)
- Belavadi and Chukwu: "Experimental Study of the Parameters Affecting Cutting Transportation in a Vertical Wellbore Annulus", paper SPE 27880 presented at the Western Regional Meeting held in Long Beach, California, 23–25 March, 1994.
- Brown N. P., Bern P. A., and Weaver A., "Cleaning deviated holes: New experimental and theoretical studies", Proceedings of the

SPE/IADC Drilling Conference, p171-180, (1989).

- Enilari, Mojisola G., "Development and evaluation of various drilling fluids for slim hole wells", M.Sc. Thesis, University of Oklahoma, Norman, Oklahoma, (2005)
- Fluent, User's Guide FLUENT 6.3.26. Fluent Inc., Canonsburg, PA, (2006).
- Ford, J.T., Peden, J. M., Oyeneyin, E. G., and Zarrough, R., "Experimental Investigation of Drilled Cuttings Transport in Inclined Boreholes", SPE 20421, Presented at the 65th Annual Technical Conference, New Orleans-Louisiana (September 23-26, (1990))
- Fordham, E. J., S. H. Bittleston and M. A. Tehrani, Viscoplastic Flow in Centered Annuli, Pipes and Slots", IEC Res. 29, 517–524 (1991).
- Han, S-M., Hwang, Y-K, Woo, N-S., Kim, Y-J., "Solid–liquid hydrodynamics in a slim hole drilling annulus", Journal of Petroleum Science and Engineering, 70, 308–319, (2010)
- Hansen, S. A., R. Rommetveit, N. Sterri, B. Aas and A. Merlo, "A New Hydraulic Model for Slim Hole Drilling Applications", Paper SPE 57579 presented at the SPE/IADC Middle East Drilling Technology Conference, Abu Dhabi, 8–10 November (1999).
- Hemphill, T. and Larsen, T. I., "Hole-Cleaning Capabilities of Oil-Based and Water-Based Drilling Fluids: A Comparative Experimental Study", SPE 26328, Presented at the 65th Annual Technical Conference and Exhibition, Houston-Texas (October 3-6, (1993))
- Hopkin, E. A.: "Factors Affecting Cuttings Removal During Rotary Drilling," paper SPE 1697 presented at the SPE-AIME 45th Annual Fall Meeting, Houston (Oct. 1970).
- Hussaini, M. S. and Azar, J. J., "Experimental study of drilled cuttings transport using common drilling muds", Society of Petroleum Engineers Journal, 23(l), ll-20, Feb. (1983).
- Karagüzel, C., Çetinel, T., Boylu, K., Çinku, F., and Çelik, M.S., "Activation of (Na, Ca)-bentonites with soda and MgO and their utilization as drilling mud", Applied Clay Science 48 (2010) 398–404
- Langlinais, J. P., A. T. Bourgoyne and W. R. Holden, Frictional, Pressure Losses for the Flow of Drilling Mud and Mud/Gas Mixtures", Paper SPE 11993 presented at the 58th Annual Technical Conference and Exhibition, San Francisco, CA, 5–8, October (1983).
- Lauzon, R. V., and Reid, K. B, "New Rheological Model Offers Field Alternative", Oil and Gas J. (May 21, 1979) 77, pp 51-57.
- Mahto, V. and Sharma, V.P. 'Characterization of Indian Bentonite Clay Samples for Water-based Drilling Fluids', Petroleum Science and Technology, 26: 15, .(2008) 1859 - 1868
- Mitsuishi, N., and Aoyagi, Y., "Non-Newtonian Fluid Flow in an Eccentric Annulus," J. Chem. Eng. Japan (1973) 6, 402-408.
- Newitt, D. M., Richardson, J. F., and Gliddon, B. J., "Hydraulic Conveying of Solids in Vertical Pipes," Trans. Inst. Chem. Eng. 39, 93-100, (1961)
- Okafor, M. N. and J. F. Evers, "Experimental Comparison of Rheology Models for Drilling Fluids," Paper SPE 24086, presented at the Western Regional Meeting, Bakersfield, OK, 30 March–11 April (1992).
- Ogugbue, C. C. E., "Non-Newtonian Power-Law Fluid Flow in Eccentric Annuli: CFD Simulation and Experimental Study", PhD

Thesis, University of Oklahoma, Norman, Oklahoma, (2009)

- Pilehvari, A., Serth, R., 2009. Generalized hydraulic calculation method for axial flow of non-Newtonian fluids in eccentric annuli. Paper SPE 111514. December SPE Drilling & Completion, 553.
- Pérez, R. M. Siquier, S. Ramírez, N. N. Müller, N. and Sáez, A. E., Non-Newtonian annular vertical flow of sand suspensions in aqueous solutions of guar gum, Journal of Petroleum Science and Engineering, Volume 44, Issues 3-4, 15 November 2004, Pages 317-331
- Pigott, R. J. S., "Mud Flow in Drilling", Drilling and Production Proceeding, API, p. 91-103. (1941)
- Sample, K. J. Bourgoyne, A.T., "Development of Improved Laboratory and Field Procedures for Determining the Carrying Capacity of Drilling Fluids," SPE Paper 7497 presented at the 53rd Annual Fall Technical Conference, Houston, Texas, Oct. 1-3, 1978.
- Sanchez, R.A., Azar, J.J., Bassal, A.A. and Martins, A.L.: "Effect of Drillpipe Rotation on Hole Cleaning During Directional-Well Drilling," SPEJ, June 1999, p.101-107.
- Sakr, M. L. H., "Turbulent flow of non-Newtonian drilling fluids in eccentric annular channels", M.Sc. thesis, Mansoura Univ., Mansoura, Egypt (2008)
- Sakr, M. L. H. Sultan, A. A, Tolba, M. A, and Badawy, M. A, "Effect of power law fluids rheology on the structure of cuttings and drilling fluid flow in wellbore eccentric annulus", to be published at Mansoura Engineering J., (2012).
- Sifferman, T. R., Myers, G. M., Haden, E. L., and Wahl, H. A.: "Drill-Cuttings Transport in Full-Scale Vertical Annuli," J. Pet. Tech. (Nov. 1974) 1295-1302.
- Tomren, P. H., lyoho, A. W. and Azar, J. J., "An Experimental Study of Cuttings Transport in Directional Wells", SPE DE, Feb. (1986), p.43-56.
- Vinod, P. S., "Effect of Fluid Rheology on Hole Cleaning in Highly-Deviated Wells", PhD thesis, RICE University, Houston, Texas June, (1994)
- Walker, S. and Li, J.: "The Effects of Particles Size, Fluid Rheology, and Pipe Eccentricity on Cuttings Transport," SPE paper 60755 presented at the 2000 SPE/ICoTA Coiled Tubing Roundtable held in Houston, TX, 5-6 April 2000.
- Wang, Zhi-ming, Guo Xiao-le, LI Ming, and Hong Yu-kui, "Effect of Drilling Rotation on Borehole Cleaning for Extended Reach Well", Journal of Hydrodynamics (2009), 21(3):366-372
- Yan, Yun-kui, Liang, Li-ping, Feng, and Wen-qiang, "Rheological study on natural heteropolysac-charide based drilling fluid", J. Cent. South Univ. Technol. (2007) s1-0188-04

Table (1)
Drilling Fluids Power Law Rheological Parameters and Density
(1-a) Bentonite Base Fluid + KCl and KF additives, Enilari (2005)

Rheological Parameters of Base Fluids with KCl.				Rheological Parameters of Base Fluids with KF.			
Fluid Composition	ρ kg/m^3	n	k (Pa.s^n)	Fluid Composition	ρ kg/m3	n	k Pa.s^n)
Base Fluid "BF"	1030.5	0.64	0.086	Base Fluid "BF"	1030.5	0.64	0.086
BF+0.5% KCl	1042.5	0.54	0.193	Base fluid + 0.5% KF	1054.5	0.39	0.594
BF+1% KCl	1066.5	0.50	0.267	Base fluid + 1% KF	1060.5	0.30	1.297
BF+ 2% KCl	1102.4	0.32	1.371	Base fluid + 2% KF	1066.5	0.23	3.538
BF+ 3% KCl	1114.4	0.18	6.037	Base fluid + 3% KF	1078.4	0.16	7.791
BF+0.5% KCl+barite to 9 ppg	1078.4	0.40	0.821	BF + 0.5% KF+ Barite to 9 ppg	1078.4	0.36	1.118
BF+0.5% KCl+ barite to 14 ppg	1677.6	0.45	1.155	BF+0.5% KF+ Barite to 14 ppg	1677.6	0.35	1.924
BF+ barite to 9 ppg	1078.4	0.58	0.133	BF+ barite to 9 ppg	1078.4	0.58	0.133
BF+barite to 14 ppg	1677.6	0.74	0.155	BF+barite to 14 ppg	1677.6	0.74	0.155

(1-b) Bentonite + PG gum, and CMC and Tylose solutions, YAN et al (2007),

Rheological Parameters Bentonite + PG gum.				Rheological Parameters KF Brines + Xanthan			
Fluid Composition	ρ kg/m^3	n	k (Pa.s^n)	Fluid Composition	ρ kg/m^3	n	k (Pa.s^n)
3% bentonite+0.5 PG gum	1012.5	0.72	0.032	3% bentonite +2 PG gum	1018.5	0.54	0.491
3% bentonite +1 PG gum	1012.5	0.64	0.110	3% bentonite +2.5 PG gum	1020.0	0.79	0.031
3% bentonite +1.5 PG gum	1018.5	0.58	0.268				

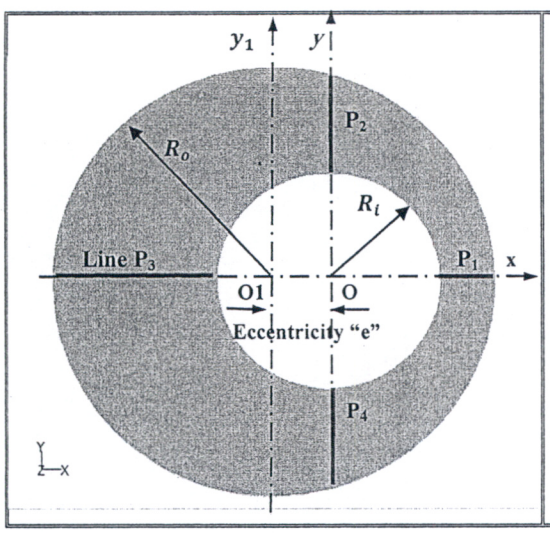

Figure (1)
The geometry of the eccentric annulus

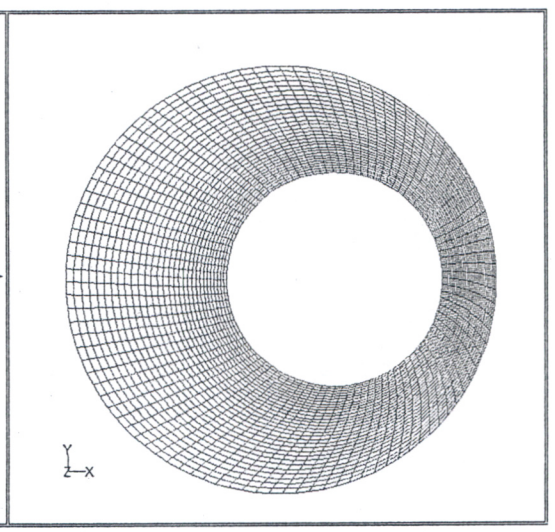

Figure (2)
The mesh structure of the eccentric annulus

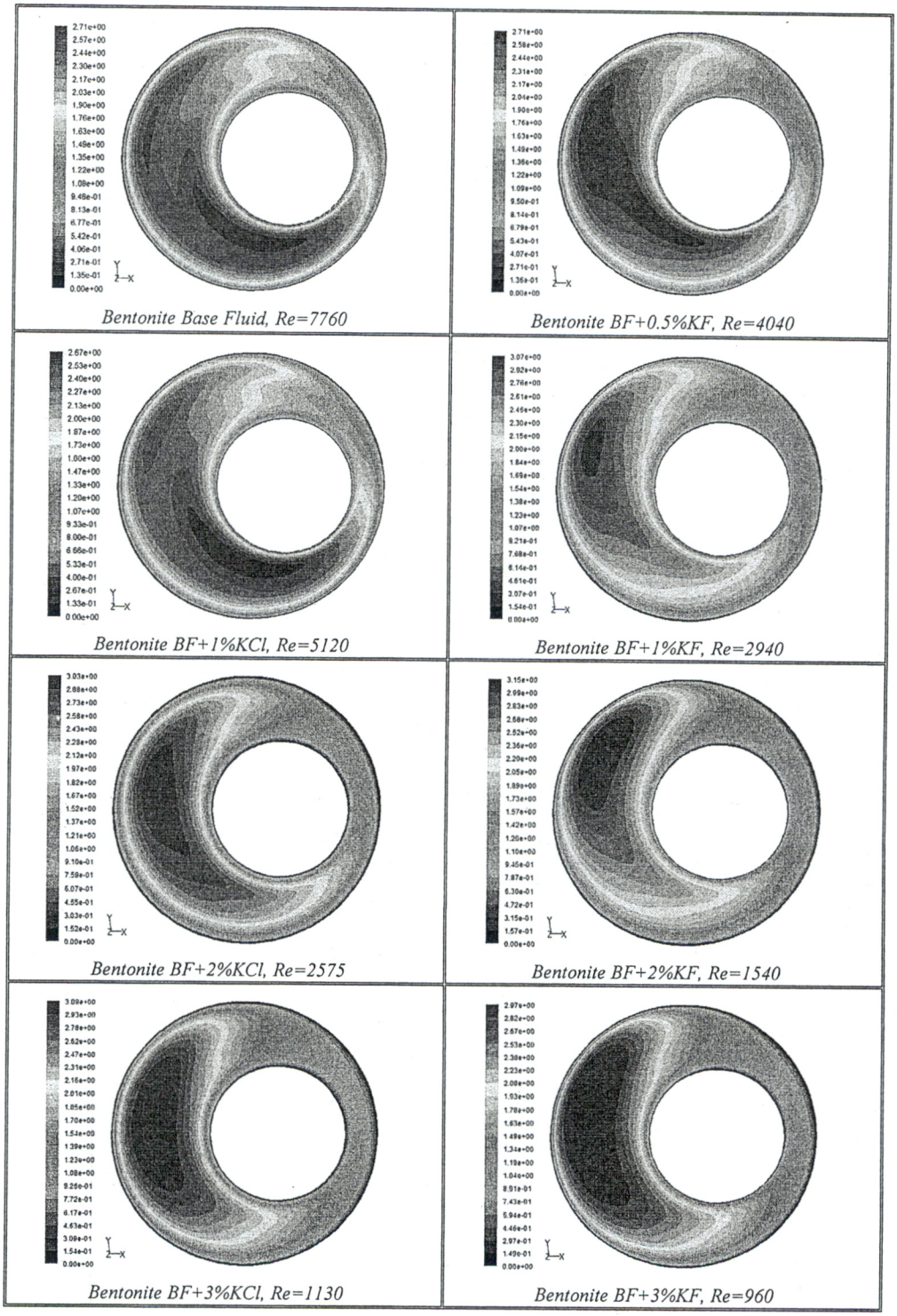

Figure (3): Axial velocity contours of the two phase flow of cuttings and bentonite base fluid with *KCl* and *KF* additives in the eccentric annulus, $U_{av} = 1.9\ m/s$, and $m_r = 50\%$, $dp = 6\ mm$

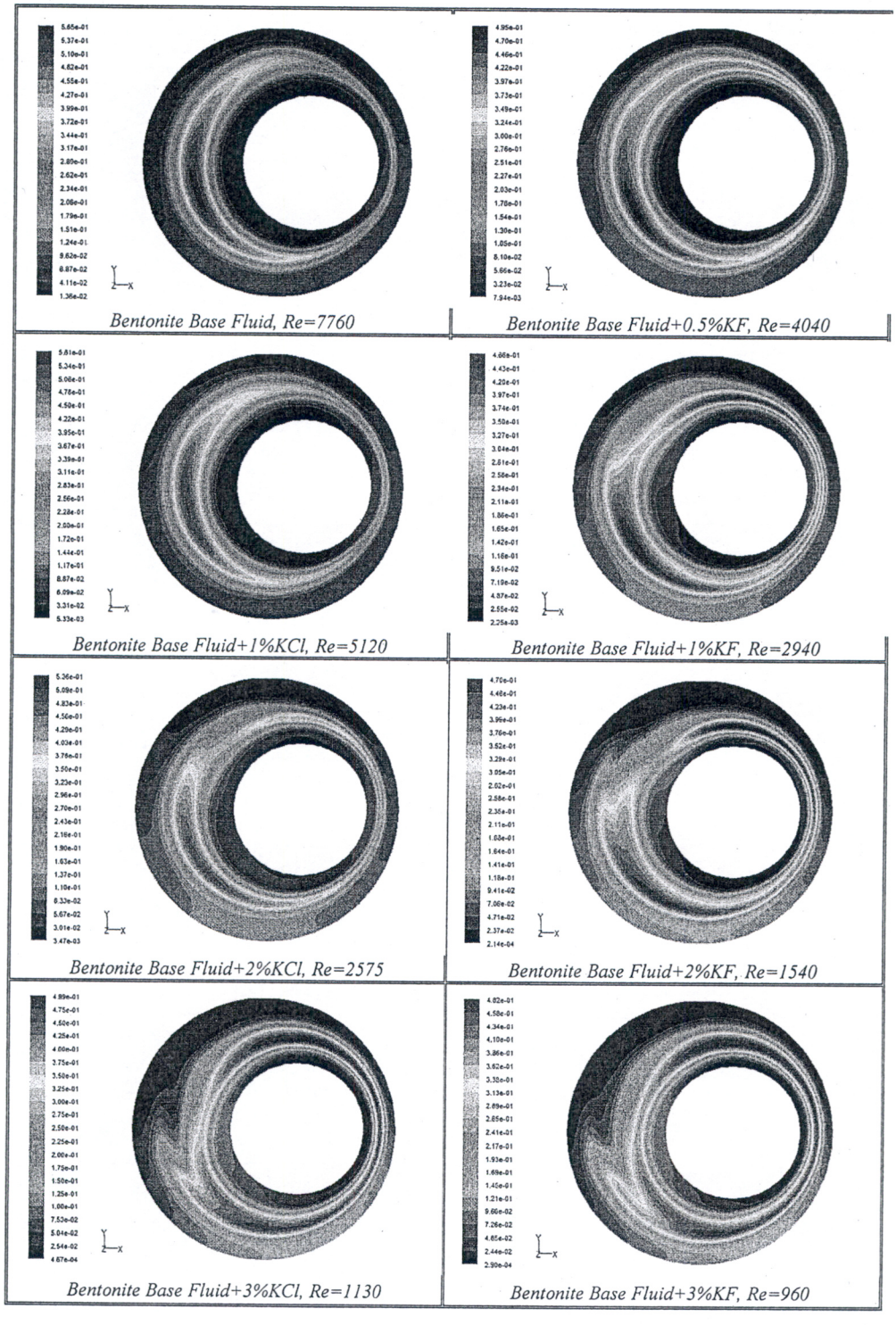

Figure (4): Cuttings volume fraction contours of the two phase flow of cuttings and bentonite base fluid with KCl and KF additives in eccentric annulus, L=5 m, $U_{av} = 1.9\ m/s$, and m_r = 50%, dp =6 mm

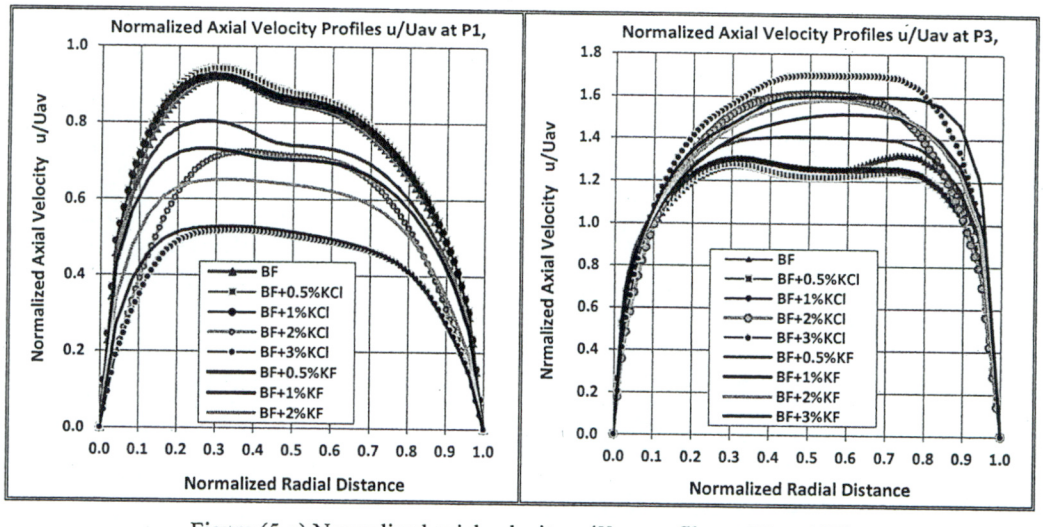

Figure (5-a) Normalized axial velocity u/U_{av} profiles at P1 and P3

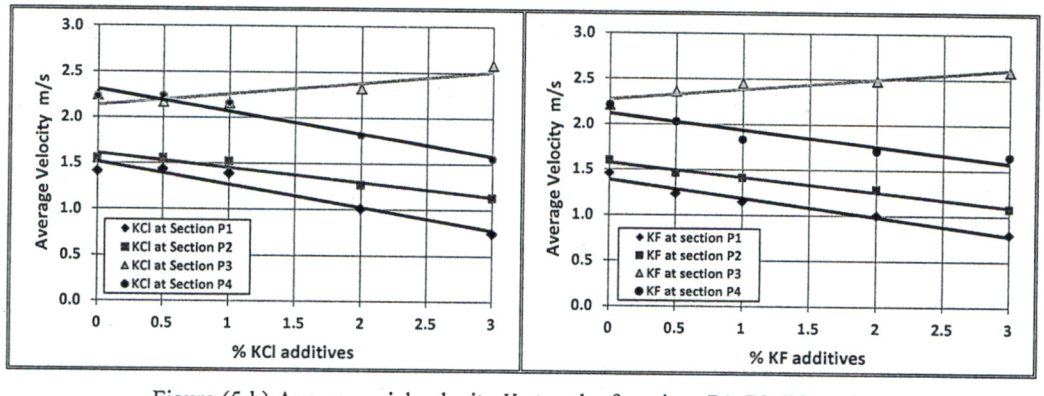

Figure (5-b) Average axial velocity U at each of sections P1, P2, P3, and P4

Figure (5): Normalized axial velocity distributions of the flow of bentonite base fluid with *KCl and KF* additives in eccentric annulus, at sections P1, P2, P3, and P4, $U_{av} = 1.9\ m/s$, and m_r = 50%, dp=6 *mm*

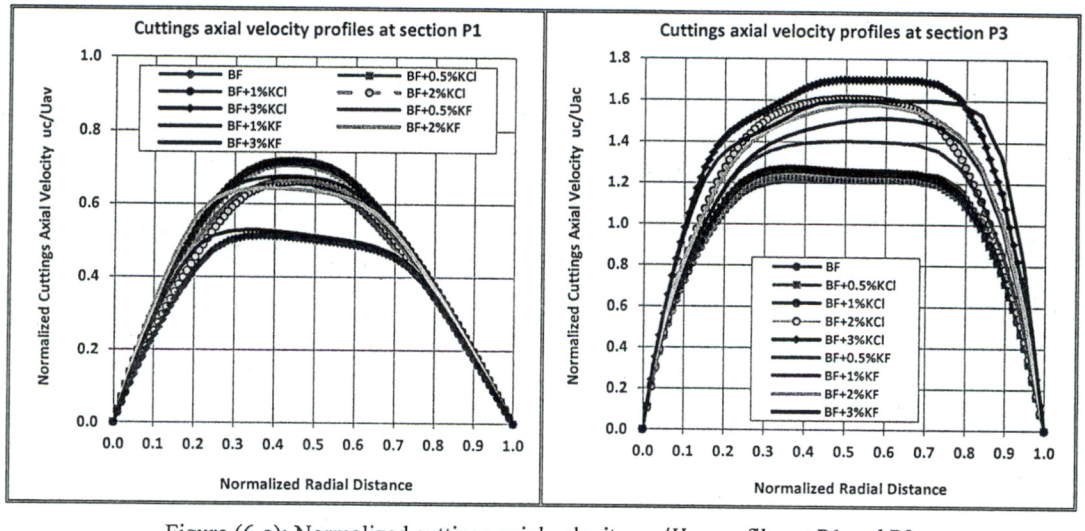

Figure (6-a): Normalized cuttings axial velocity u_c/U_{av} profiles at P1 and P3

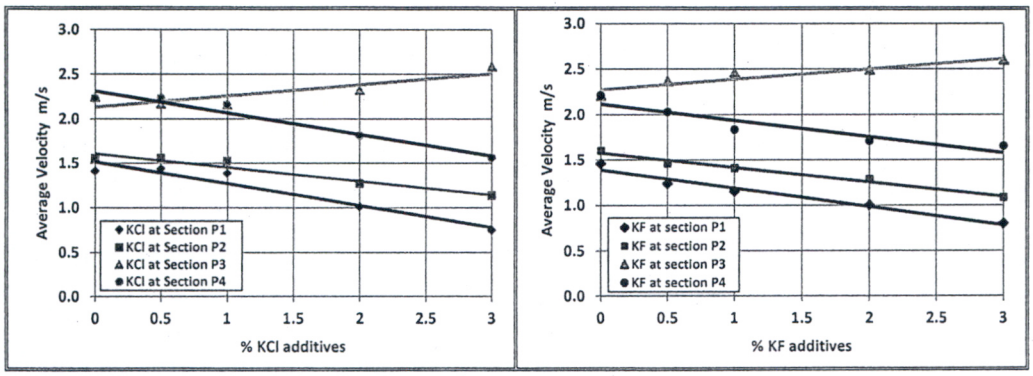

Figure (6-b) Cuttings Average Axial Velocity at each of sections P1-P4

Figure (6): Cuttings axial velocity profiles of the two phase flow of bentonite base fluid with KCl and KF additives and cuttings in eccentric annulus, L=5 m, $U_{av} = 1.9\ m/s$, and m_r =50%, dp=6 mm

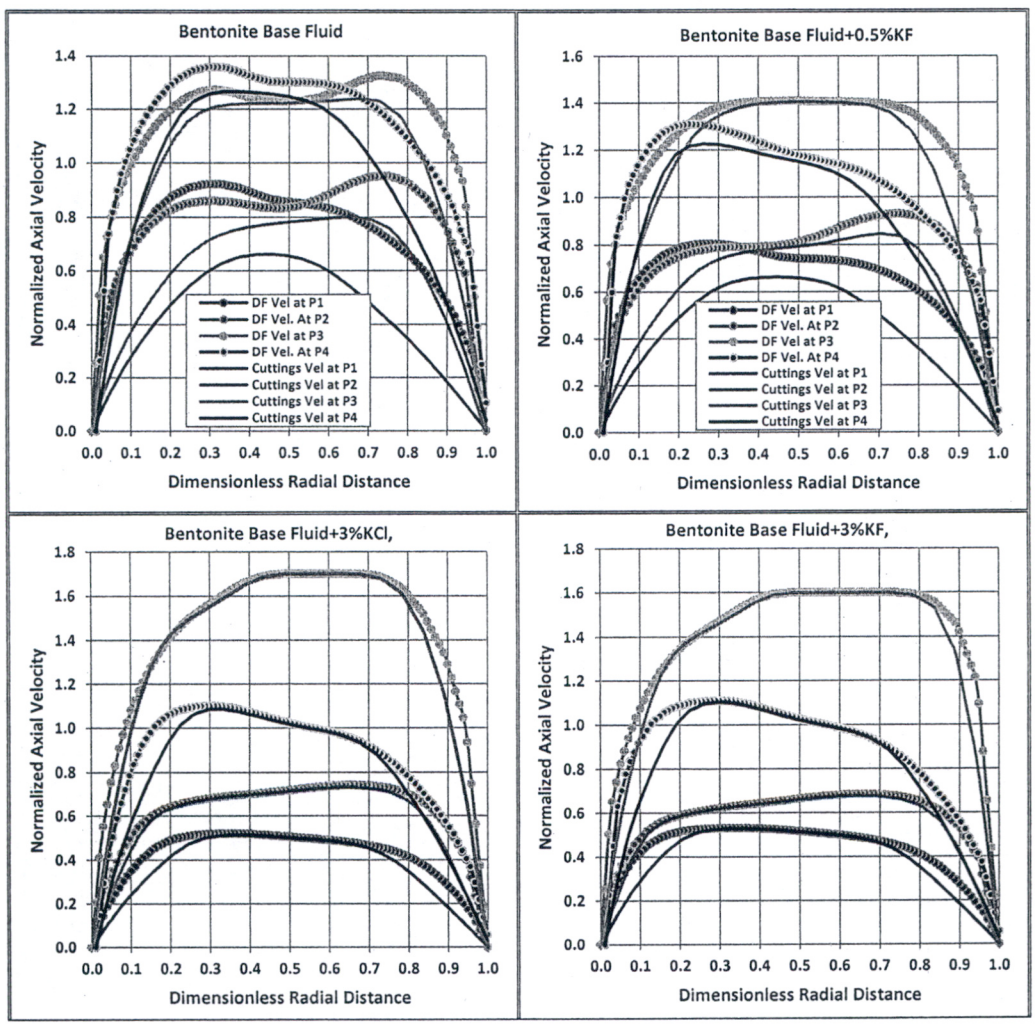

Figure (7-a): Cuttings and drilling fluid axial velocity profiles in eccentric annulus at sections *P1-P4*,

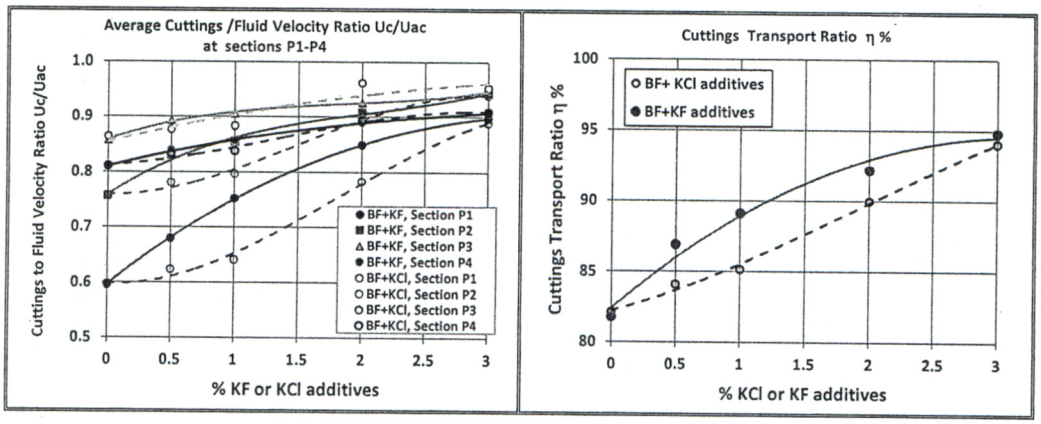

Figure (7-b) Average Cuttings/Fluid axial velocity at P1-P4, and Cuttings transport ratio

Figure (7): Cuttings and drilling fluid axial velocity profiles in eccentric annulus at sections *P1-P4*, Bentonite mud with *KCl and KF* additives, $U_{av} = 1.9\ m/s$, and m_r = 50%, dp=6 mm

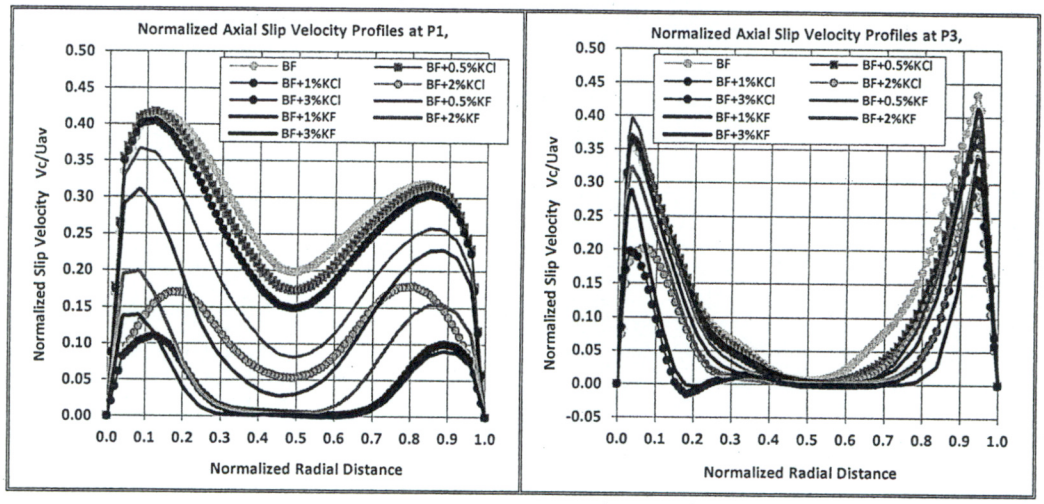

Figure (8-a) normalized slip velocity v_s profiles of drilled cuttings at sections P1 and P3

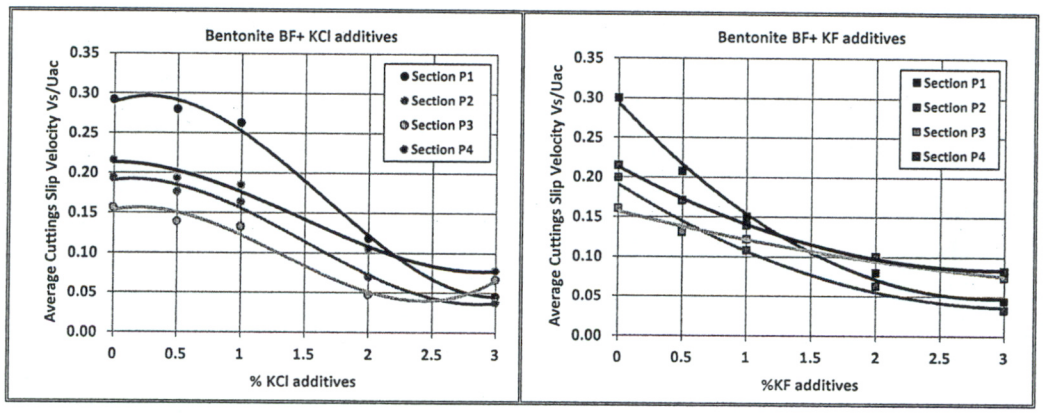

Figure (8-b) Averaged normalized slip velocity of cuttings as function of *KCl* and *KF* additives

Figure (8): Cuttings slip velocity Vs profiles of bentonite base fluid with KCl and KF additive flow in eccentric annulus, $U_{av} = 1.9\ m/s$, and m_r =50%, dp=6 mm.

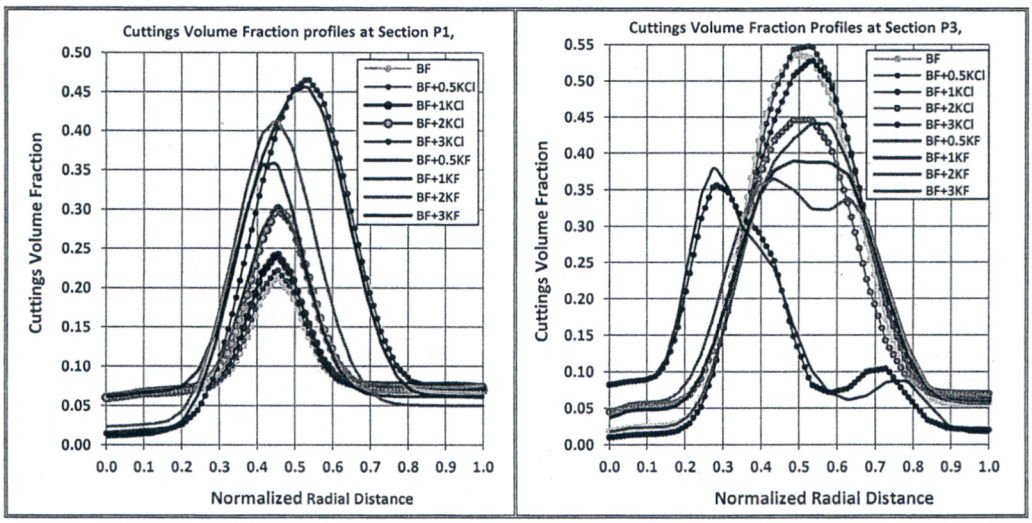

Figure (9-a) Cuttings Volume Fraction profiles at narrow and wide gap sections P1 and P3

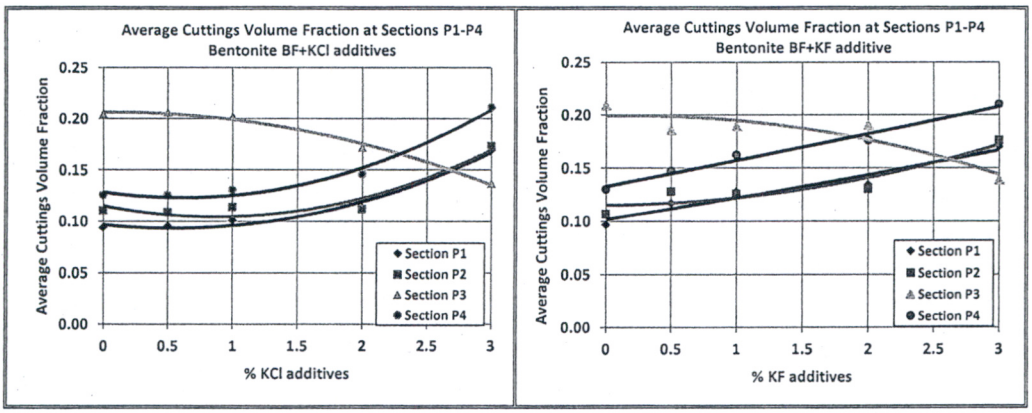

Figure (9-b) Cuttings averaged volume fraction at P1-P4 as function *KCl* and *KF* additive

Figure (9): Cuttings volume fraction profiles in two phase flow of cuttings and bentonite base fluid with *KCl* and *KF* additive flow in eccentric annulus, L=5 m, $U_{av} = 1.9\ m/s$, and m_r =50%, dp=6 mm.

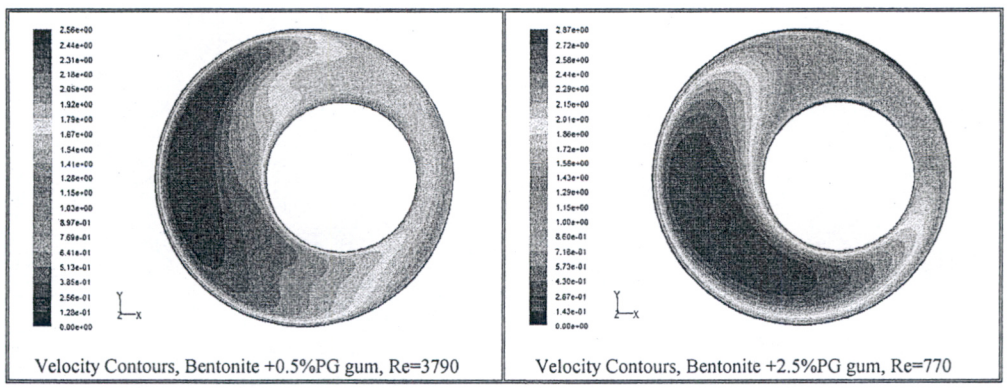

Figure (10-a): Axial velocity contours of bentonite with PG gum additive flow

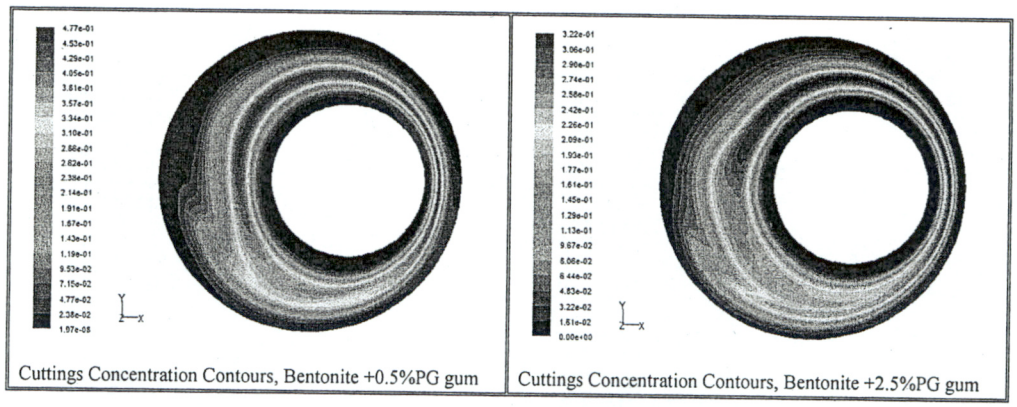

Figure (10-b): Cuttings volume fraction contours of bentonite with PG gum additive

Figure (10): Axial velocity contours and Cuttings volume fraction contours of bentonite with PG gum additive flow in eccentric annulus, L=5 m, $U_{av} = 1.9\ m/s$, mr=40% and dp=4 mm

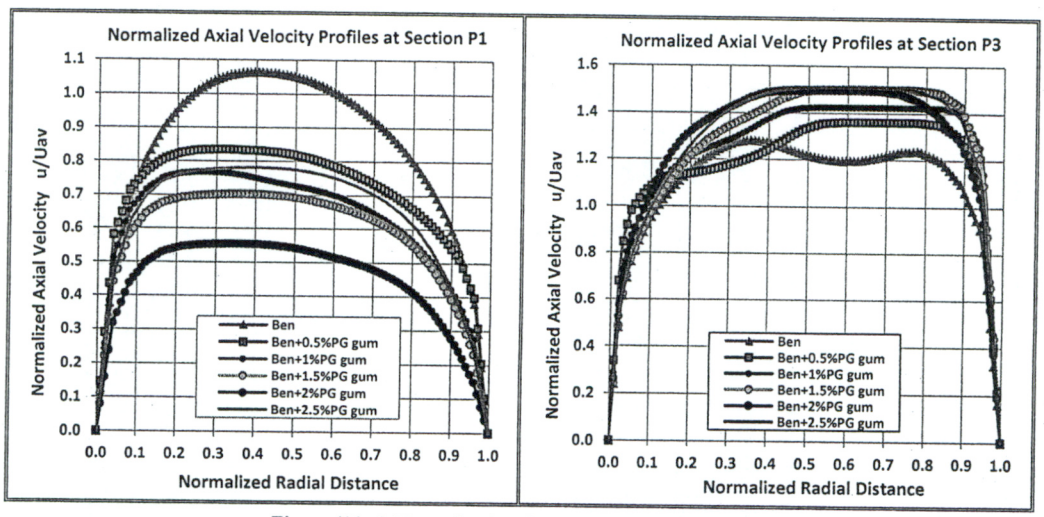

Figure (11-a) Normalized Axial Velocity Profiles u/U_{av}

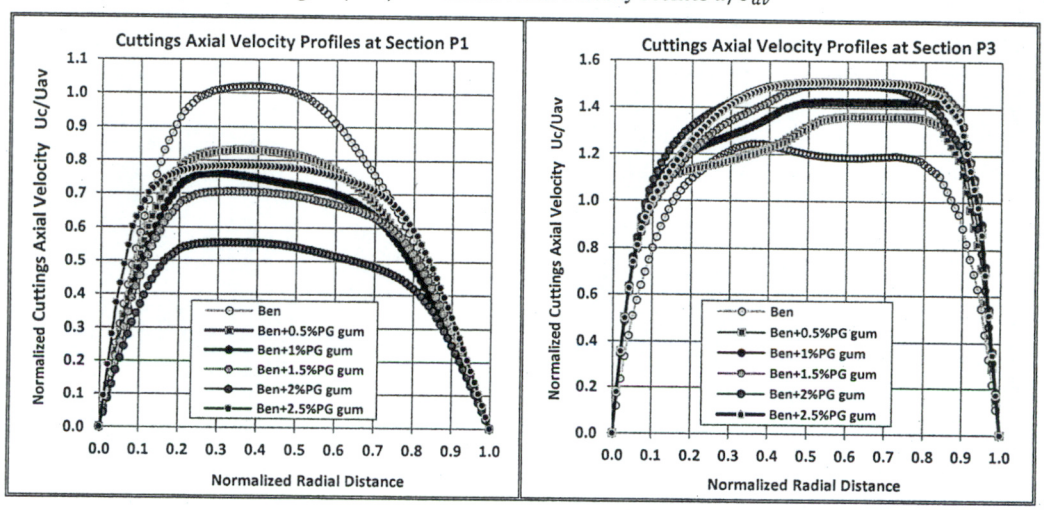

Figure (11-b) Normalized Cuttings Axial Velocity Profiles u_c/U_{av}

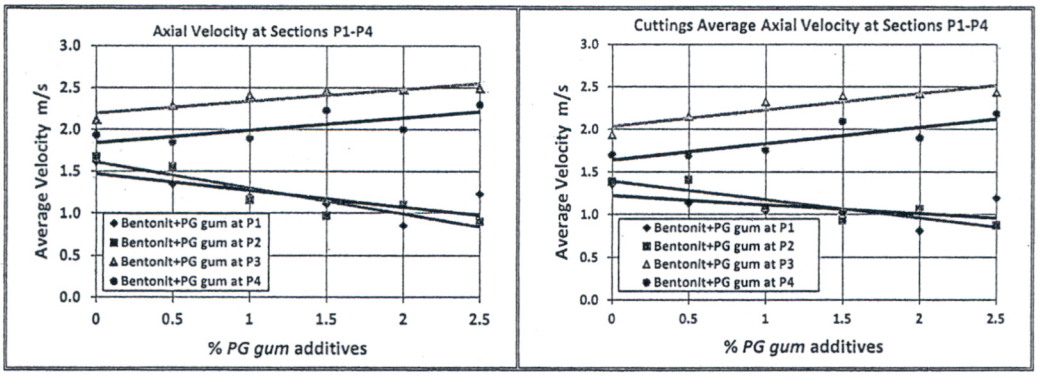

Figure (11-c) Drilling Fluid and Cuttings average axial velocity at Sections P1-P4 as function of *PG gum*

Figure (11): Drilling Fluid and Cuttings axial velocity profiles of 3% bentonite with *PG gum* flow in the eccentric annulus, L=5 m, U_{av}=1.9 m/s, mr=40%, dp=4 mm

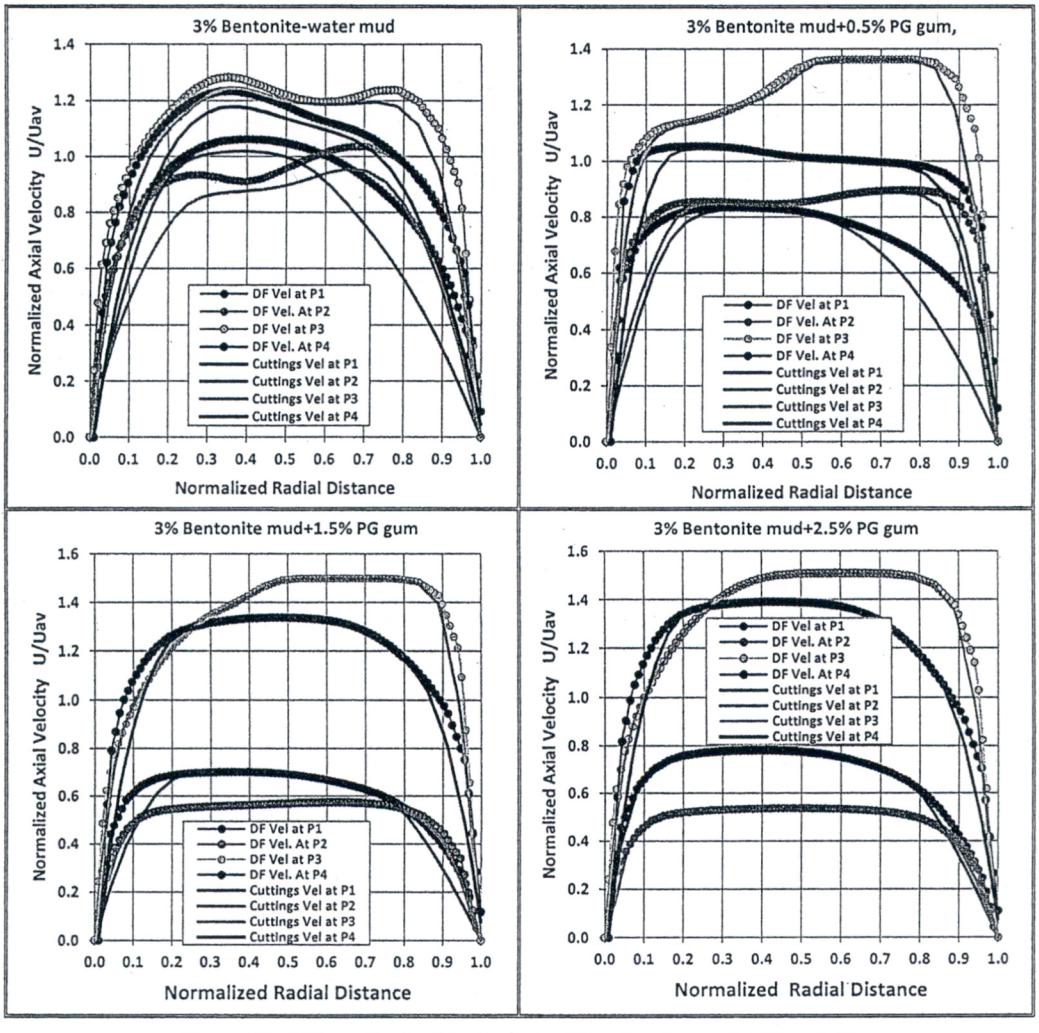

Figure (12-a) Normalized axial velocity profiles of cuttings and drilling fluid

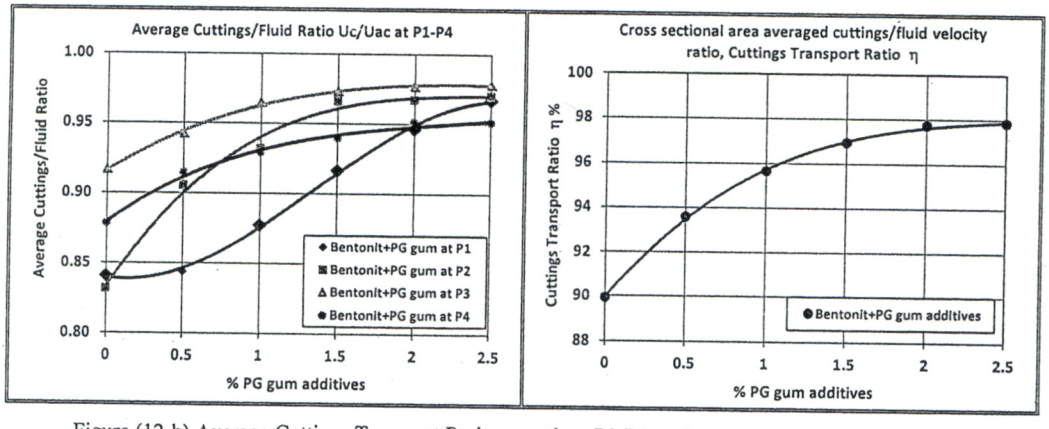

Figure (12-b) Average Cuttings Transport Ratio at sections P1-P4, and at the eccentric annulus section

Figure (12): Cuttings axial velocity profiles and fluid axial velocity profiles of 3% bentonite with *PG gum* flow in eccentric annulus, L=5 m, U_{av}=1.9 m/s, mr=40%, dp=4 mm

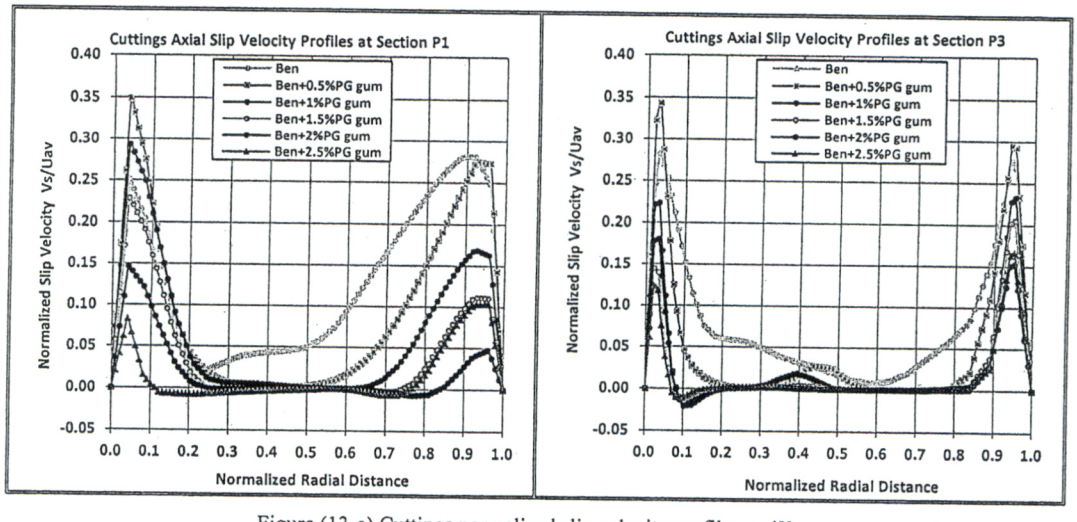

Figure (13-a) Cuttings normalized slip velocity profiles v_s/U_{av}

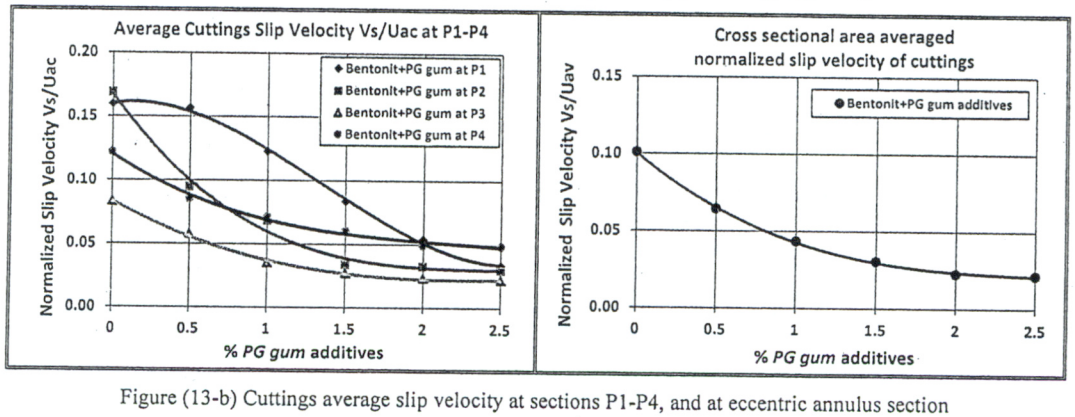

Figure (13-b) Cuttings average slip velocity at sections P1-P4, and at eccentric annulus section

Figure (13): Normalized cuttings slip velocity profiles of 3% bentonite with *PG gum* flow in eccentric annulus, L=5 m, U_{av}=1.9 m/s, mr=40%, dp=4 mm

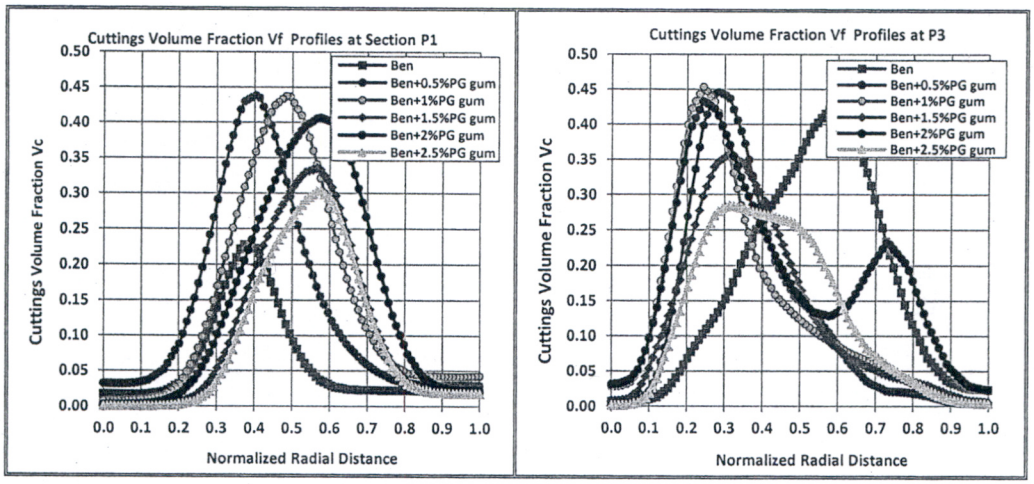

Figure (14): Cuttings slip velocity profiles of 3% bentonite-water mud with PG gum additive flow in eccentric annulus, L=5 m, $U_{av} = 1.9\ m/s$, and m_r =40%, dp=4 mm.

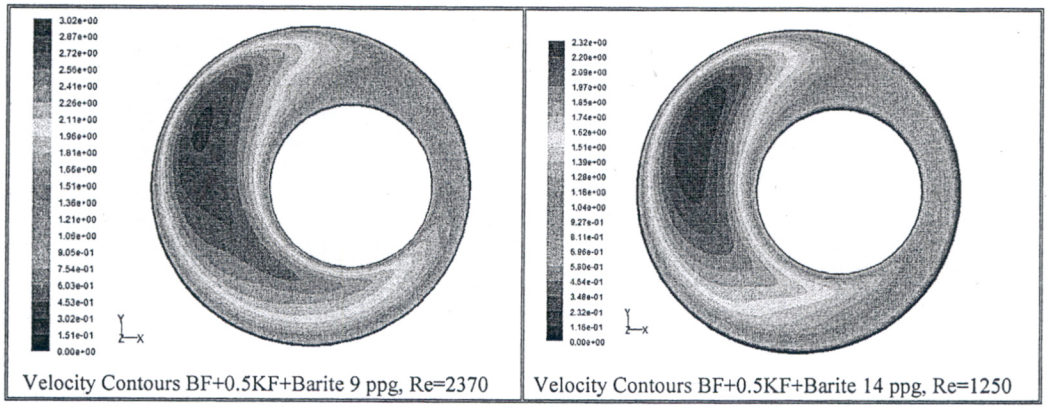

Figure (15-a) axial velocity contours

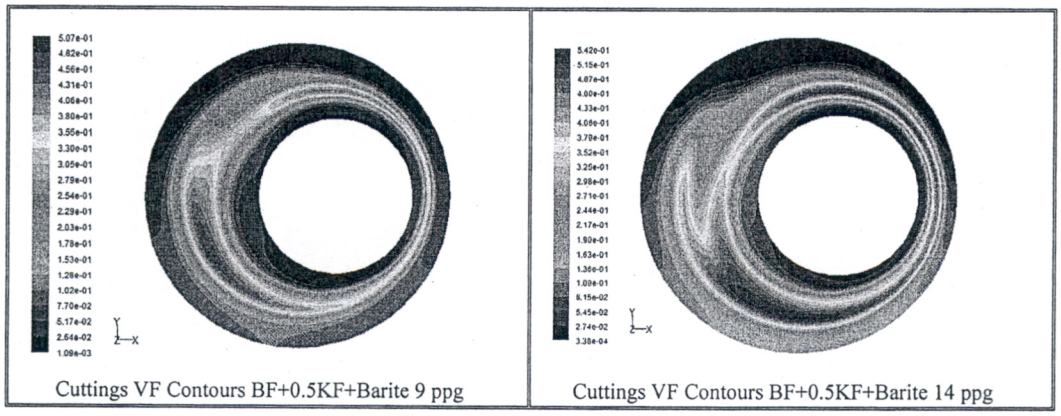

Figure (15-b) Cuttings volume fraction contours

Figure (15): Effect of barite additives on axial velocity contours and cuttings volume fraction contours of *KF* bentonite mud flow in eccentric annulus, L=5, $U_{av} = 1.9\ m/s$, mr=50% and dp=6 mm

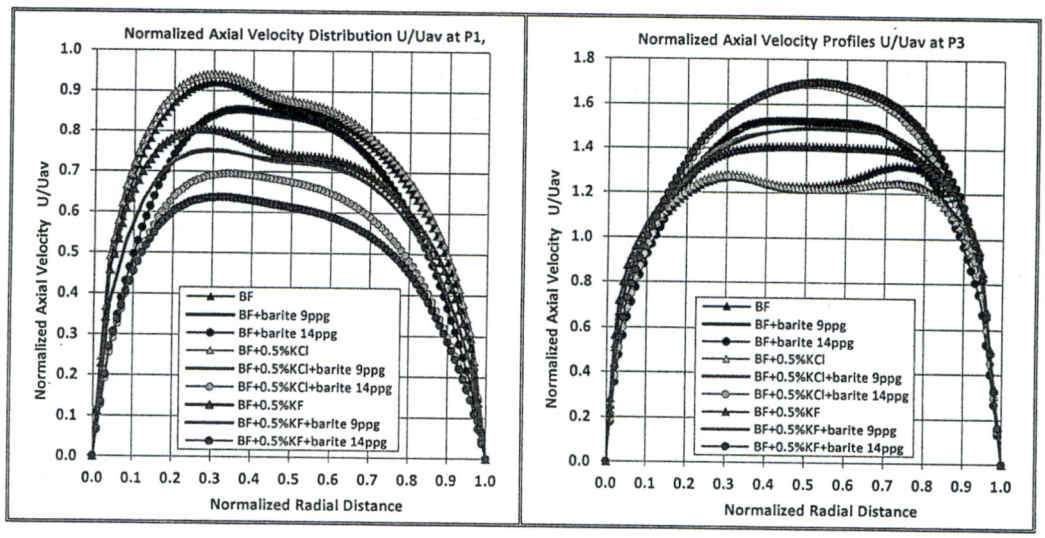

Figure (16-a) Axial velocity profiles of drilling fluid at sections *P1and P3*

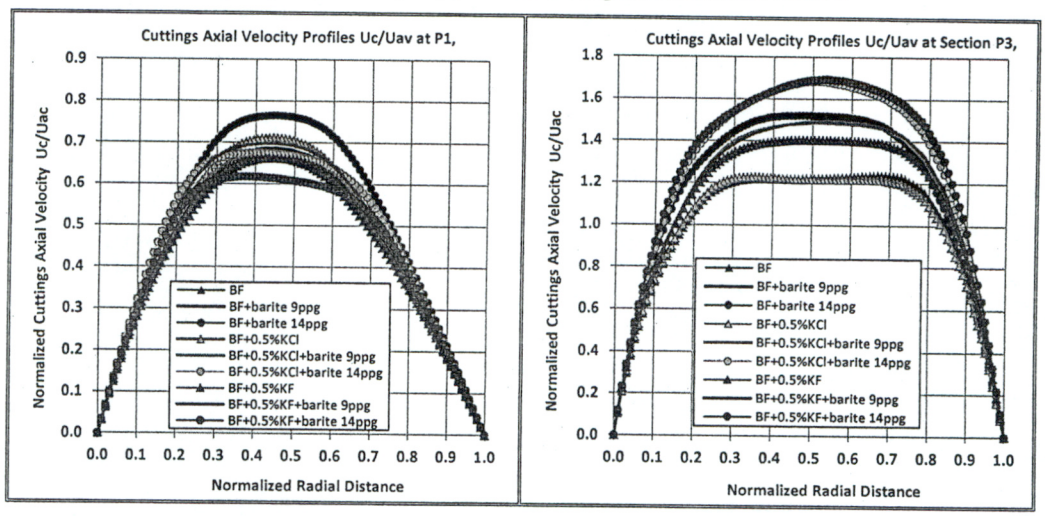

Figure (16-b) Axial velocity profiles of cuttings at sections *P1and P3*

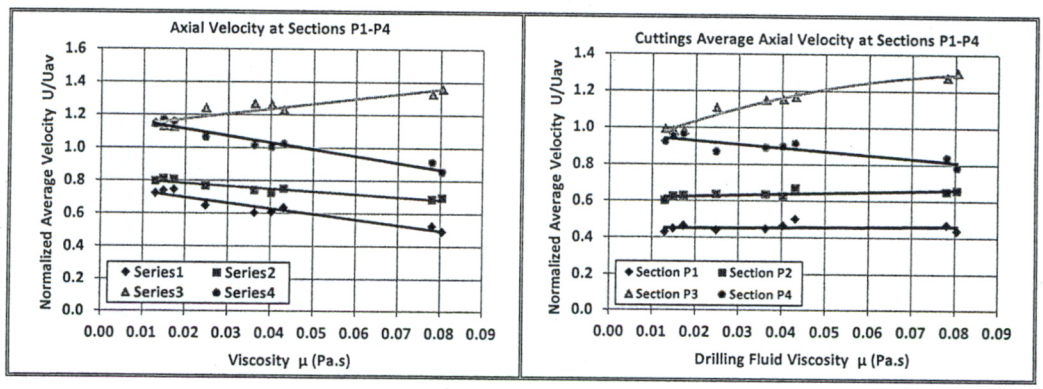

Figure (16-c) Average axial velocity of drilling fluid and cuttings at sections *P1-P4*

Figure (16): Effect of barite additives on axial velocity of drilling fluids and cuttings of *KCl and KF* bentonite mud flow in eccentric annulus, L=5, U_{av} =1.9 m/s, mr=50% and dp=6 mm

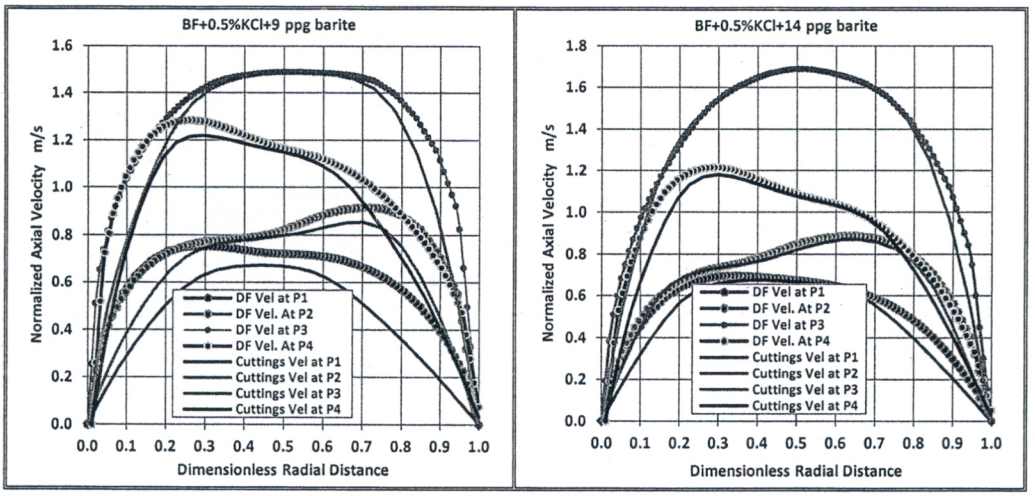

Figure (17-a) Comparison between Cuttings velocity profiles and fluid velocity profiles

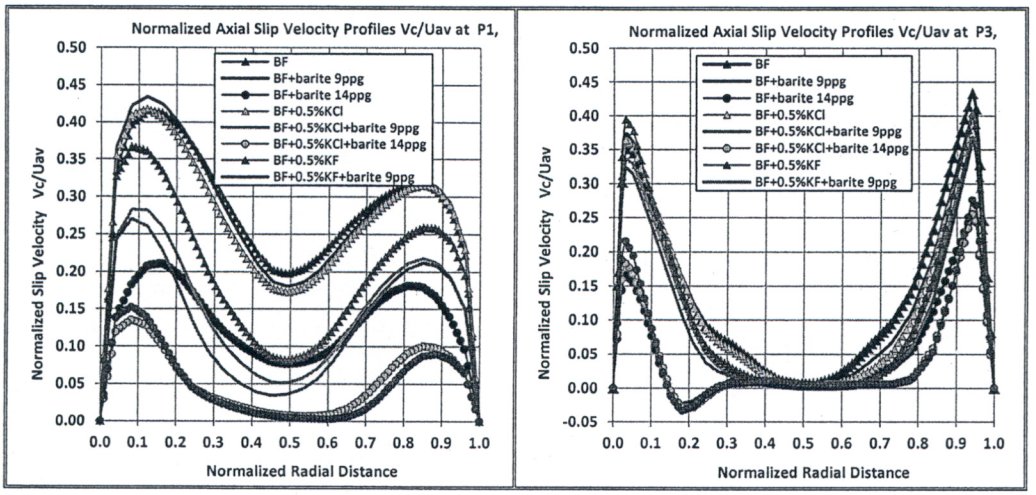

Figure (17-b) Normalized slip velocity profiles

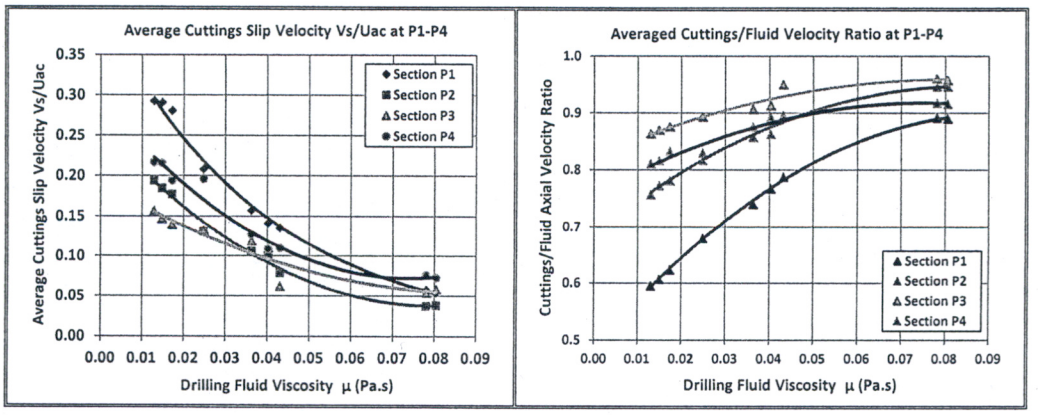

Figure (17-c) Averaged cuttings slip velocity and Average cuttings/fluid velocity ratio

Figure (18): Effect of *barite* additive on cuttings/drilling fluid velocity profiles and cuttings slip velocity profiles of *KCl and KF bentonite* flow in eccentric annulus, L=5 m, U_{av}=1.9 m/s, mr=50%, dp=6 mm

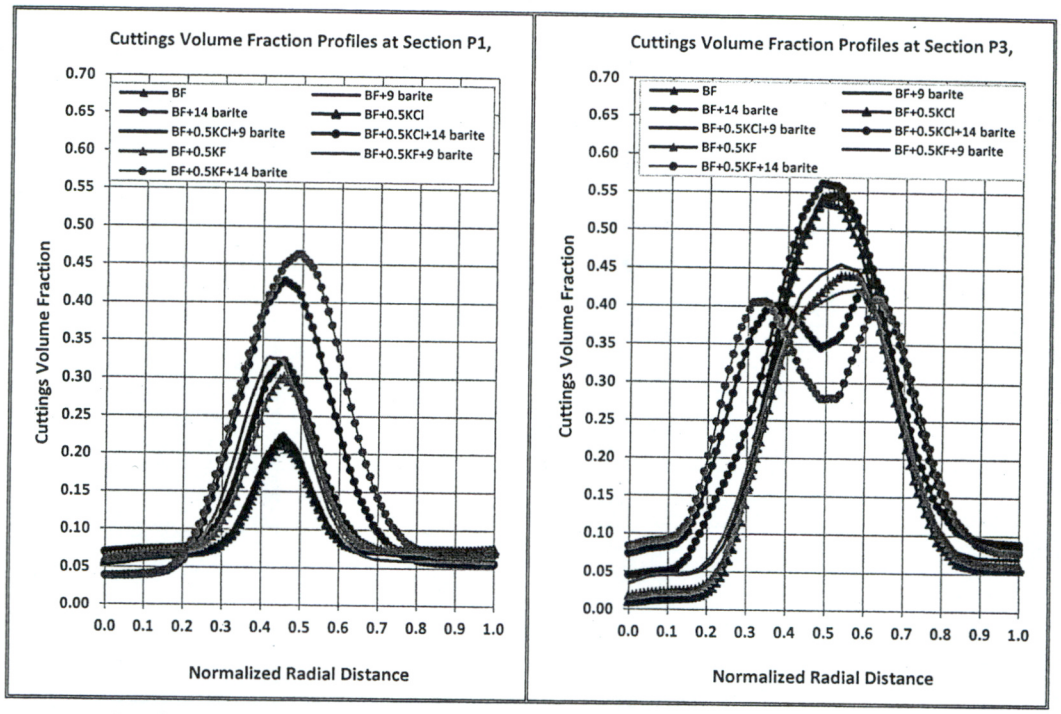

Figure (18): Effect of *barite* additive on cuttings volume fraction profiles of *KCl and KF bentonite* flow in eccentric annulus, L=5 m, U_{av}=1.8 m/s, mr=50%, dp=6 mm

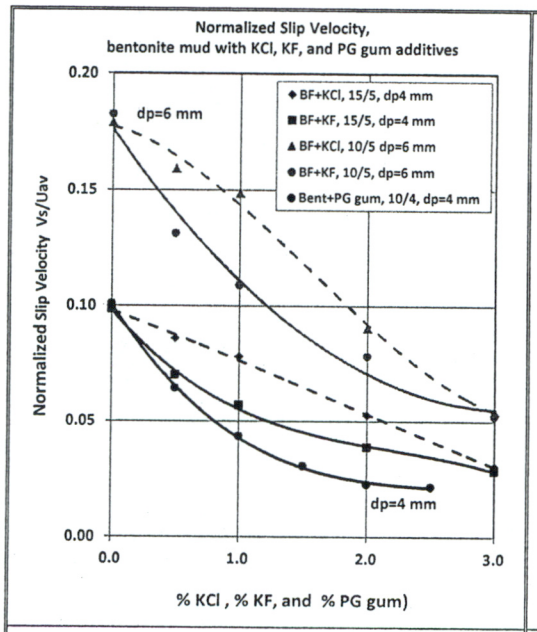

Figure (19-a) Slip Velocity

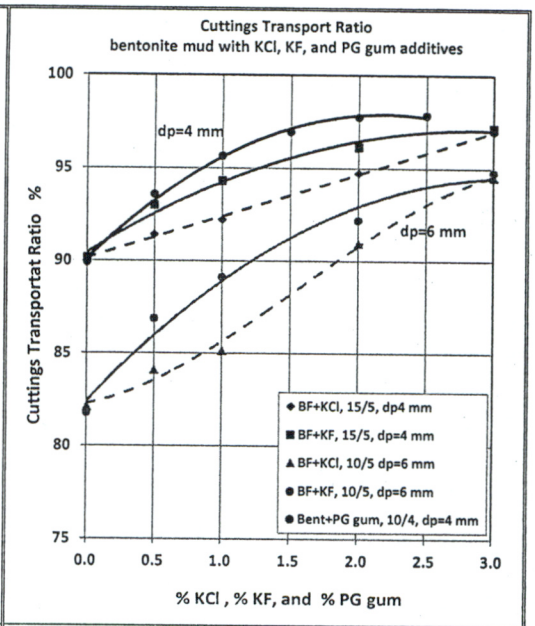

Figure (19-b) Cuttings Transport Ratio

Figure (19): Effect of drilling fluid additives on slip velocity and cuttings transport ratio of bentonite mud flow in eccentric annulus

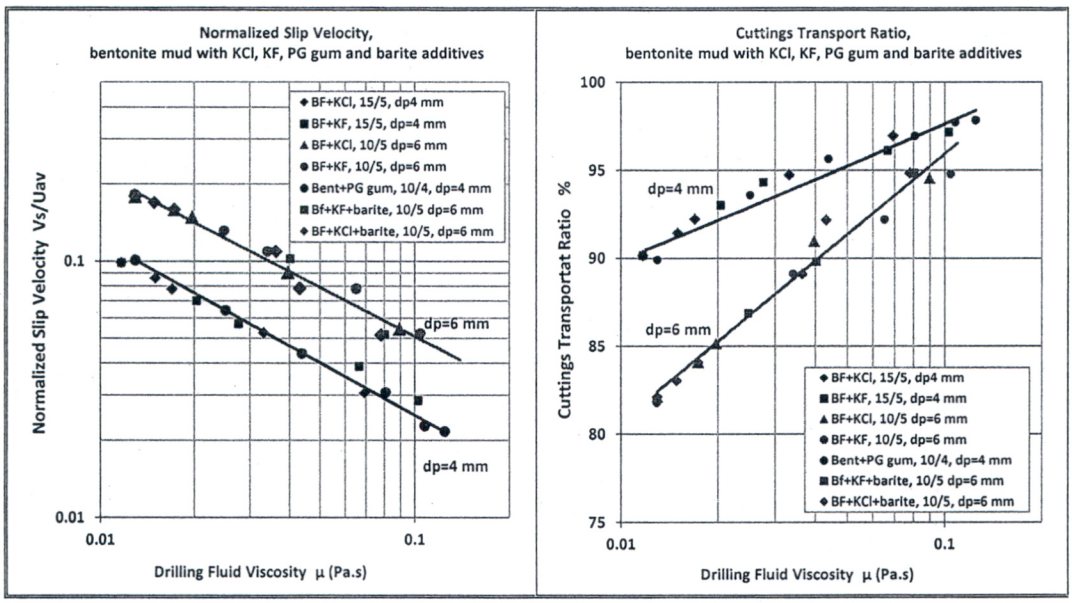

Figure (20-a) Slip Velocity

Figure (20-b) Cuttings Transport Ratio

Figure (20) Effect of drilling fluid additives on slip velocity and cuttings transport ratio of bentonite mud flow in eccentric annulus

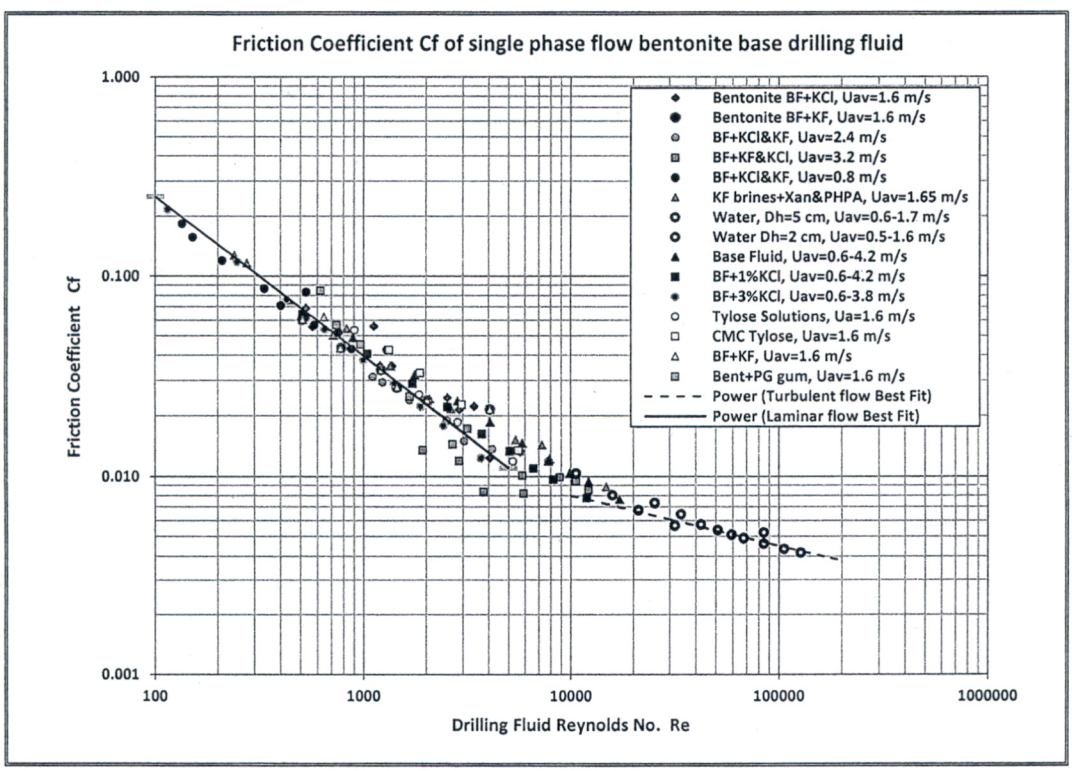

Figure (21-a) Friction Coefficient of the single phase flow of drilling fluids in eccentric annulus as function of Reynolds No Re

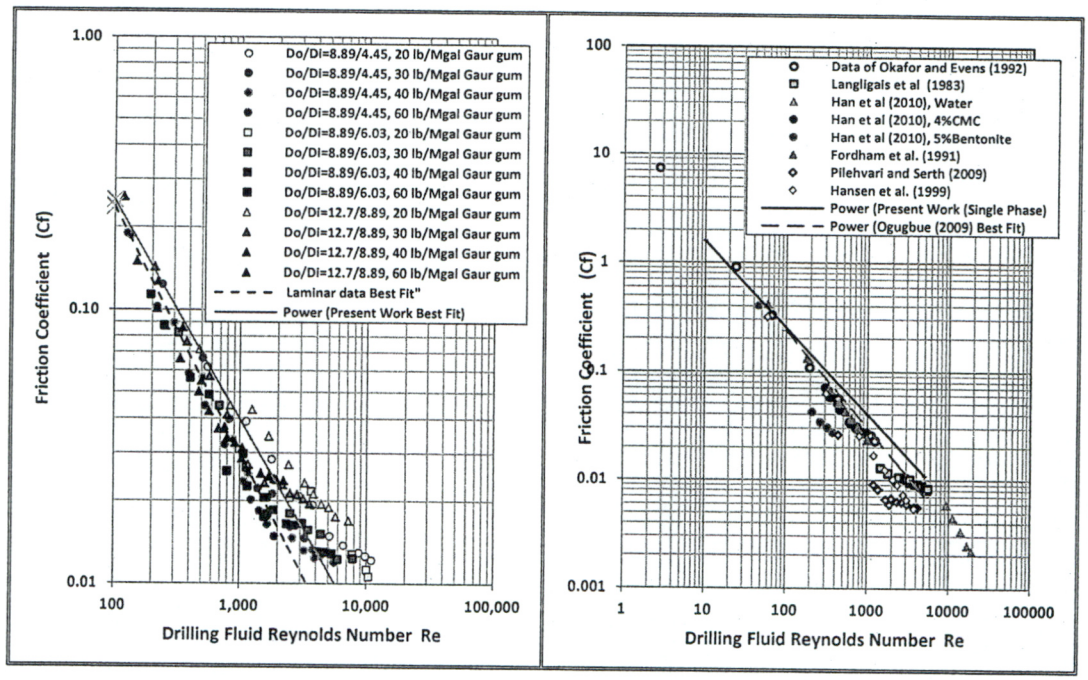

Figure (21-b) Comparison of Friction Coefficient of the single phase flow of bentonite base muds in eccentric annulus with available experimental data

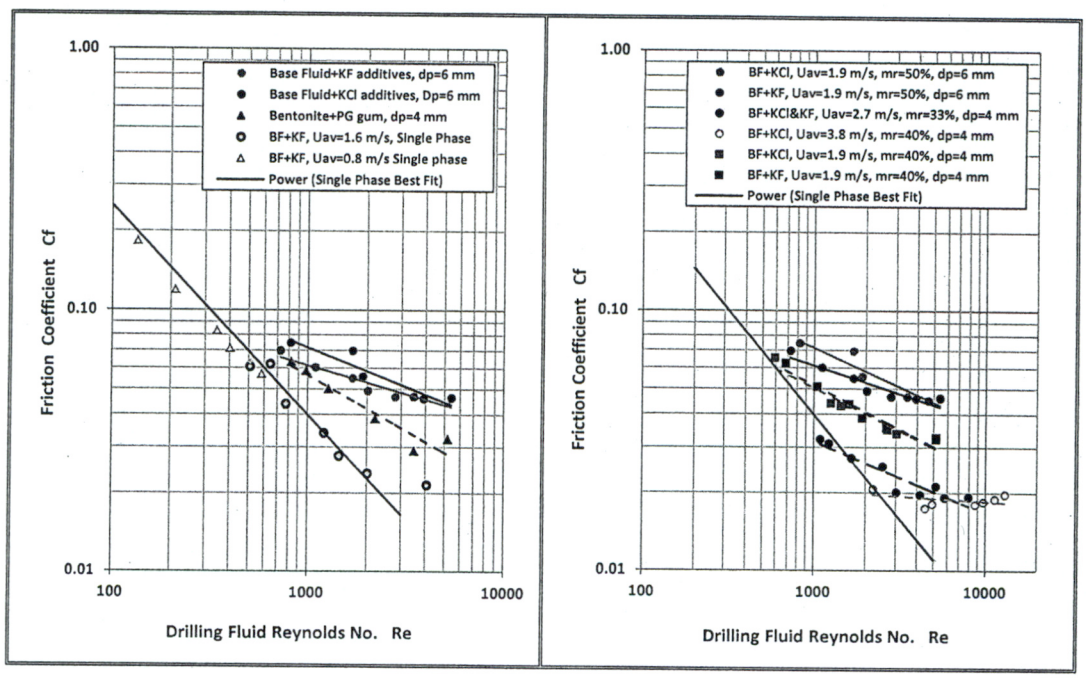

Figure (22) Friction Coefficient of the two phase flow of drilled cuttings and bentonite base drilling fluids with additives in eccentric annulus as function of Reynolds No Re